Neuronal downregulation of *PLCG2* impairs synaptic function and elicits Alzheimer disease hallmarks

Audrey Coulon[1]†, Florian Rabiller[1]†, Mari Takalo[2]†, Avishek Roy[3]†, Henna Martiskainen[2]†, Dolores Siedlecki-Wullich[1], Tiago Mendes[1], Celia Lemeu[1], Lukas-Iohan Carvalho[1], Anaël Ehrardt[3], Ana Raquel Melo de Farias[1], Marc Hulsman[4-7], Chloé Najdek[1], Nina Lannette-Weimann[1], Alejandra Freire-Regatillo[1], Philippe Amouyel[1], Camille Charbonnier[8], Orio Dols-Icardo[9,10], Heli Jeskanen[2], Roosa-Maria Willman[2], Teemu Kuulasmaa[2], Mitja Kurki[11], John Hardy[12], Richard Wagner, Sami Heikkinen[2], Henne Holstege[4-7], Petra Mäkinen[2], Gaël Nicolas[13], Simon Mead[14], Michael Wagner[15,16], Alfredo Ramirez[15-19], Tuomas Rauramaa[20], Aarno Palotie[11], Rebecca Sims[21], Hilkka Soininen[22], John van Swieten[23], Julie Williams[21], Céline Bellenguez[1], Benjamin Grenier-Boley[1], Carla Gelle[1], Erwan Lambert[1], Anne-Marie Ayral[1], Florie Demiautte[1], Marcos R. Costa[1,24], Séverine Deforges[3], Devrim Kilinc[1], Christophe Mulle[3]‡ Julien Chapuis[1]‡, Mikko Hiltunen[2]‡, Julie Dumont[1]‡[#], Jean-Charles Lambert[1]‡[#]

[1] Univ. Lille, Inserm, CHU Lille, Institut Pasteur de Lille, U1167 - RID-AGE - Facteurs de risque et déterminants moléculaires des maladies liées au vieillissement, Lille, France

[2] Institute of Biomedicine, University of Eastern Finland, Kuopio, Finland

[3] Interdisciplinary Institute for Neuroscience, CNRS UMR 5297, University of Bordeaux, Bordeaux, France

[4] Genomics of Neurodegenerative Diseases and Aging, Human Genetics, Vrije Universiteit Amsterdam, Amsterdam UMC location VUmc, Amsterdam, the Netherlands

[5] Alzheimer Center Amsterdam, Neurology, Vrije Universiteit Amsterdam, Amsterdam UMC location VUmc, Amsterdam, the Netherlands

[6] Amsterdam Neuroscience, Neurodegeneration, Amsterdam, the Netherlands

[7] Delft Bioinformatics Lab, Delft University of Technology, Delft, the Netherlands

[8] Univ Rouen Normandie, Inserm U1245 and CHU Rouen, Department of Biostatistics and CNRMAJ, F-76000 Rouen, France

[9] Department of Neurology, II B Sant Pau, Hospital de la Santa Creu i Sant Pau, Universitat Autonota de Barcelona, Barcelona, Spain

[10] Biomedical Research Networking Center on Neurodegenerative Diseases, National Institute of Health Carlos III, Madrid, Spain

[11] Institute for Molecular Medicine Finland, University of Helsinki, Helsinki, Finland.

[12] Reta Lila Weston Research Laboratories, Department of Molecular Neuroscience, University College London Institute of Neurology, London, UK

[13] Univ Rouen Normandie, Inserm U1245 and CHU Rouen, Department of Genetics and CNRMAJ, F-76000 Rouen, France

[14] Medical Research Council Prion Unit at University College London, University College London Institute of Prion Diseases, London, UK

[15] Department of Cognitive Disorders and Old Age Psychiatry, University Hospital Bonn, Medical Faculty, Bonn, Germany

[16] German Center for Neurodegenerative Diseases, Bonn, Germany

[17] Division of Neurogenetics and Molecular Psychiatry, Department of Psychiatry and Psychotherapy, Faculty of Medicine and University Hospital Cologne, University of Cologne, Cologne, Germany

[18] Department of Psychiatry and Glenn Biggs Institute for Alzheimer's and Neurodegenerative Diseases, San Antonio, TX, USA

[19] Cologne Excellence Cluster on Cellular Stress Responses in Aging-Associated Disease (CECAD), University of Cologne, Cologne, Germany

[20] Department of Pathology, Kuopio University Hospital, Kuopio, Finland and Unit of Pathology, Institute of Clinical Medicine, University of Eastern Finland, Kuopio, Finland
[21] Medical Research Council Centre for Neuropsychiatric Genetics and Genomics, Division of Psychological Medicine and Clinical Neuroscience, School of Medicine, Cardiff University, Cardiff, UK
[22] Department of Neurology, University of Eastern Finland, Kuopio, Finland
[23] Department of Neurology, Erasmus Medical Centre, Rotterdam, the Netherlands
[24] Brain Institute, Federal University of Rio Grande do Norte, Natal, Brazil
† Contributed equally as co-first author
‡ Contributed equally as co-last author
[#] Address correspondence to: julie.dumont@univ-lille.fr, jean-charles.lambert@pasteur-lille.fr

ABSTRACT

We developed a high content screening to investigate how Alzheimer disease (AD) genetic risk factors may impair synaptic mechanisms in rat primary neuronal cultures. Out of the gene targets identified, we found that shRNA-mediated downregulation of *Plcg2* in mouse dentate gyrus neurons consistently impaired dendritic morphology and synaptic function. In human neuronal cultures (hNCs), *PLCG2* downregulation also impaired synaptic function and was associated with increased levels of Aβ and Tau phosphorylation, potentially *via* the AKT/GSK3β axis. Very rare *PLCG2* loss-of-function (LoF) variants were associated with a 10-fold increased AD risk. *PLCG2* LoF carriers exhibit low mRNA/protein *PLCG2/*PLCγ2 levels, consistent with nonsense-mediated mRNA decay mechanisms. Restoring PLCγ2 levels in shPLCG2-hNCs fully reversed the disease-related phenotypes. Our findings indicate that the downregulation of PLCγ2 increases the risk of AD by impairing synaptic function and increasing the levels of Aβ and Tau phosphorylation in neurons.

Key words: Alzheimer's disease, *PLCG2*, synapse, high-content screening, patch-clamp, iPSCs, GSK3β, Tau, microelectrode arrays

INTRODUCTION

Alzheimer's disease (AD) is characterized by intracellular aggregation of abnormally hyperphosphorylated Tau protein and extracellular accumulation of amyloid-beta (Aβ) in plaques. According to the "amyloid cascade hypothesis", Aβ aggregation is an early toxic condition that can induce Tau aggregation and neuronal death. However, while recent clinical studies using anti-Aβ therapies in principle support this hypothesis (*1*), it has been regularly modified to reflect the advancements in our understanding of AD (*2, 3*, *4*). It is now well accepted that the amyloid cascade hypothesis appears to be over-simplistic and fails to account for the intricacy and heterogeneity of the pathophysiological processes involved in the common forms of the disease.

Since the proportion of risk attributable to genetic susceptibility factors for AD has been estimated to be between 60% and 80% in twin studies (*5*), defining the AD genetic component has been considered as a means of gaining a better understanding of the pathophysiological processes and generating complementary or alternative hypotheses. The development of genome-wide association studies (GWASs) and high-throughput sequencing has considerably advanced the AD genetic landscape over the last fifteen years, leading to the characterization of 76 loci associated with the AD risk (*6–8*). Based on this new genetic landscape of AD, we and others developed parallel approaches employing systematic post-GWAS studies. Beyond inflammation processes, we also proposed synaptic fragility/sensitivity as a pathological trigger, depending on genetic risk factors, some of which have already been linked to synaptic mechanisms, such as BIN1, FERMT2, PTK2B or CD2AP. (*9–12*). This notion fits with key clinical observations suggesting that synapse dysfunction/loss is (i) one of the earliest pathological hallmarks in the brain before hippocampal neuronal death and (ii) the strongest marker of cognitive decline (for a review, see (*13–15*)). Within this background, we systematically addressed the potential implication of the genes located in the loci associated with AD risk (as reported in (*6*)) in synaptic mechanisms. For this purpose, we developed a high-content screening (HCS) approach to systematically analyze the impact of the downregulation of a large number of AD risk genes on synaptic density and to reveal the potential implication of these genes in synaptic function.

RESULTS

HCS identifies GWAS-defined genes as potential modulators of synapse density

We developed a HCS approach to systematically characterize the effect on synaptic density of 198 genes located in the 76 loci associated with AD risk and selected as being expressed in brain cells (according to publicly available RNAseq datasets, see Material and Methods). A lentiviral shRNA library targeting these 198 genes was developed. The screen was performed in 384-well plates using rat hippocampal primary neuronal cultures (PNCs) transduced at day 1 in vitro (DIV1) using two multiplicities of infection (MOI 2 and 4, **Fig. 1a, b**). Immunocytochemistry was conducted at DIV21 against Synaptophysin 1 (Syp), Homer1 and Map2, pre-synaptic, post-synaptic and somatodendritic markers, respectively (**Fig. 1d, e**) (*16*). Synaptic density was then assessed via a high-content analysis workflow by assigning each post-synaptic structure to the nearest pre-synaptic structure, as previously described (*17*). Non-targeting shRNA (shNT) and shRNA against Syp (shSyp) were used as controls. The complete HCS results are presented in **Table S1**. We selected AD risk genes with the strongest effect on synaptic density (top and bottom 2.5%) in three independent experiments, resulting in five genes (*Usp6nl*, *Psmc3*, *Plcg2*, *Csnk1g1*, *Cyb561*) associated with lower synaptic density and four genes (*Snx1*, *Ica1l*, *Oplah* and *Nck2*) associated with higher synaptic density when downregulated (**Fig. 1c**). For these

nine genes, we confirmed the impact of shRNA-mediated downregulation on protein levels in PNCs (**Fig. 1f, g**). In conclusion, HCS allowed us to identify several genes located within the loci associated with AD risk that strongly modulate synaptic density in rat PNCs.

GWAS-defined genes, including *Plcg2*, impact electrophysiological properties of PNCs

We first determined whether proteins encoded by the nine selected genes could be detected in synaptosomes purified from PNCs (**Fig. S1**). Except for Cyb561 (data not shown), we detected their presence in the PSD95 and/or non-PSD95 fractions. We then analyzed the impact of their downregulation on the electrophysiological properties of mature PNCs (at DIV21) using multielectrode arrays (MEAs). As a positive control, the downregulation of *Syp* showed significant decreases in the mean spike and burst frequencies, two read-outs for neuronal activity (**fig. 1h** and **1i,** respectively). Similarly, the downregulation of *Usp6nl* and *Plcg2* significantly decreased the mean spike and burst frequencies. These results are of particular interest since *Plcg2* was believed to be almost only expressed in microglia and, as a consequence, this AD risk gene was almost exclusively investigated in this cell type (*18*–*21*). Thus, we focused on *Plcg2*, which is also expressed in glutamatergic neurons as evidenced by publicly available single nuclei RNA sequencing (snRNA) datasets from mouse hippocampus (*22*), human brain (*23*) and snRNAseq datasets generated in-house using human brain organoids (*24*)(**Fig. S2**).

***Plcg2* downregulation in the mouse dentate gyrus reduces dendritic arborization complexity and spine density of granule cells**

Plcg2/PLCG2 is highly expressed in the mouse and human dentate gyrus (DG) (*25*), which is the main gateway from the entorhinal cortex inputs to the hippocampus. Synaptic plasticity in the DG is strongly affected in mouse models of AD (*26*, *27*). Lentiviral vectors encoding either an shRNA against *Plcg2* (LV-shPLCG2) or a non-targeting control shRNA (LV-shNT), combined with GFP were injected in the dorsal hippocampus of adult mice of both sexes in the ipsi- (LV-shPLCG2) and contra-lateral (LV-shNT) hemispheres, respectively (**Fig. 2a and Fig. S3**). An analysis on GFP fluorescence images of DG neurons from shNT (n=35 neurons) and shPLCG2 (n=42 neurons) injected mice (**Fig. 2b)** revealed that *Plcg2* downregulation resulted in a reduction in dendritic length (shNT = 148±12 µm *vs* shPLCG2 = 77±9 µm; $p<0.001$), dendritic volume (shNT = 270±32 μm^3 *vs* shPLCG2 = 87±5 μm^3; $p<0.001$, **Fig.2c, d**) and in the number of intersections in a Sholl analysis (($p<0.0001$; intersection vs. distance from soma $F_{(24, 1560)}=23.23$) **(Fig. 2g, h),** but not in the complexity index ($p=0.24$) or total branch number ($p=0.52$) **(Fig. 2e, f)**. We observed a decrease in the density and morphology of dendritic spines in shPLCG2-transduced DG granule cells (number of spines per µm: shNT = 0.70±0.04, n=73 neurites *vs* shPLCG2 = 0.27±0.01, n=75 neurites; $p<0.0001$), and an alteration of their morphology with decreased head diameter (shNT = 0.48±0.02 µm, n=100 *vs* shPLCG2 = 0.29±0.01 µm, n=103; $p<0.0001$), and spine length (shNT = 0.73±0.06 µm, n=89 *vs* shPLCG2 = 0.53±0.05 µm, n=101; $p<0.0001$; **Fig. 2j, l**). In conclusion, consistently with our results *in vitro*, *Plcg2* downregulation markedly impairs neuronal dendritic morphology and spine density in DG granule cells *in situ*.

***Plcg2* downregulation in the mouse dentate gyrus impairs electrophysiological properties of granule cells**

We then prepared slices for the electrophysiological recording of DG granule cells transduced with shPLCG2 or shNT as visualized and targeted by their GFP fluorescence (**Fig. 3a**). We assessed the intrinsic electrophysiological properties (shNT, n=15 cells; shPLCG2, n=13 cells; **Fig. 3b, f; Fig. S4b**).

Plcg2 downregulation led to a reduction of the input resistance (shNT = 570±79 MOhm *vs* shPLCG2 = 312±35 MOhm; p=0.0061; **Fig. 3d**) and of the firing threshold (shNT = –64.4±3.2 mV *vs* shPLCG2 = –71.4±0.8 mV; p=0.009) which was accompanied with an increase in the half-width of action potentials (shNT = 1.17 ms *vs* shPLCG2 = 1.25 ms; p=0.027, Mann-Whitney test; **Fig. S4c, d**). We found that the amount of current required for the cell to fire an action potential (the rheobase) was significantly higher following *Plcg2* downregulation (shNT = –57±11 pA *vs* shPLCG2 = –86±10 pA; p=0.022) (**Fig. 3c**). The number of spikes triggered by depolarizing pulses as a function of the amplitude of current injected also showed that shPLCG2-transduced DG neurons were less excitable ($F_{(1, 588)}$ = 10.87; df=1; p=0.001, ordinary 2-way ANOVA) (**Fig. 3g**). Overall, *Plcg2* downregulation leads to a substantial decrease in input resistance and in neuronal excitability. It can be suggested that Plcg2 contributes to the regulation of voltage-dependent ion channels around resting membrane potential of DG granule cells. We then performed voltage-clamp recordings in the presence of tetrodotoxin (TTX; 500 nM) to assess the impact of *Plcg2* downregulation on spontaneous miniature excitatory post-synaptic currents (mEPSCs) (mEPSCs) (**Fig. 3h**). We found significant differences in the average frequency of mEPSCs between shNT (n=27) and shPLCG2 (n=15) transduced neurons (shNT = 0.47±0.07 Hz *vs* shPLCG2 = 0.27±0.08 Hz; p=0.026; **Fig. 3i**). This result is consistent with the observed reduction of spine density. In addition, *Plcg2* downregulation resulted in a decrease of the amplitude of mEPSCs (shNT = 13.6±0.7 pA *vs* shPLCG2 = 10.8±0.5 pA; p=0.034; cumulative distribution of mEPSC amplitudes, p=0.0008, Kolmogorov-Smirnov test**; Fig. 3j, k)**. In conclusion, in accordance with our results *in vitro*, *Plcg2* downregulation markedly impairs electrophysiological properties of DG granule cells.

Downregulation of PLCγ2 in human neuronal cultures negatively impacts synaptic density and function

We then sought to extend our findings in rodents to *in vitro* model of human neurons, derived from human induced pluripotent stem cells (iPSCs). After 4 weeks of spontaneous differentiation from neural progenitor cells, transduced with either a non-targeting control shRNA (shNT) or a shRNA targeting *PLCG2* (shPLCG2), we obtained a mixed culture of mature human induced neurons and astrocytes, which we will refer to as human neuronal cultures (shNT-hNCs or shPLCG2-hNCs; **Fig. 4a**). We validated via immunoblotting that PLCγ2 downregulation in this mixed culture was specific as it did not impact PLCγ1 expression (**Fig. 4b**). To characterize the impact of *PLCG2* downregulation on synaptic density in hNCs, we used custom microfluidic devices in which mature neuronal synapses can be fluidically isolated in a distinct (synaptic) chamber and easily quantified. As in the case of HCS, we performed immunocytochemistry against synaptic markers and assessed synaptic density using a previously described algorithm (*17*) (**Fig. 4c**). We fully replicated in hNCs the results obtained in the HCS experiments using rat NPCs, *i.e.*, *PLCG2* downregulation decreased synaptic density (**Fig. 4c-d**). Similar results were obtained when using rat PNCs cultured in microfluidic devices (**Fig. S5**). Lastly, we analyzed the impact of *PLCG2* downregulation on the electrophysiological properties of hNCs using MEAs. Again, we replicated in hNCs the results we obtained in rat PNCs, *i.e.*, *PLCG2* downregulation induced a significant decrease in spike and burst frequencies (**Fig. 4e**). In conclusion and in accordance with our results observed in the rodent brain, *PLCG2* downregulation impacts synaptic density and function *in vitro* in hNCs.

Downregulation of PLCγ2 in human neuronal cultures increases both TAU phosphorylation and the levels of Aβ

We next tested the potential impact of *PLCG2* downregulation in hNCs on the different hallmarks of

AD, *i.e.*, amyloid precursor protein (APP) metabolism and quantity/phosphorylation state of Tau. In shPLCG2-hNCs, a significant increase in both APP (**Fig. 4f, g**) and Aβ levels (**Fig. 4h**) was detected. *PLCG2* downregulation was also associated with a strong increase in Tau phosphorylation at multiple epitopes (**Fig. 4f, i**). To note, an increase in total Tau protein levels was also detected (**Fig. 4f, g**). We finally investigated whether the impact of *PLCG2* downregulation on Tau hyperphosphorylation could be mediated through the regulation of ERK1/2, GSK3β, p38/MAPK and AKT kinases, known regulators of Tau phosphorylation (**Fig. 4k, l)**. No difference in the total protein levels or phosphorylation status of ERK1/2 or p38/MAPK was observed when *PLCG2* was downregulated. However, *PLCG2* downregulation increased the level of phosphorylated GSK3β at Y216 and decreased the level of phosphorylated AKT at S473 (**Fig. 4l**). Both epitope sites are indicative of the active forms of the kinases. Altogether, these data indicate that *PLCG2* downregulation is associated with increased Aβ level, and Tau phosphorylation, potentially *via* the AKT/GSK3β axis.

Rare *PLCG2* loss-of-function variants are associated with an increase in AD risk

Importantly, our above-mentioned data suggest that the *PLCG2* downregulation may be deleterious and favor the development of AD through synaptic impairment and increased Aβ levels and Tau hyperphosphorylation. Therefore, we postulated that loss-of-function (LoF) variants responsible for a univocal reduction in *PLCG2/*PLCγ2 expression/activity might be associated with an increased risk of AD. To address this possibility, we first used two independent whole exome sequencing (WES) datasets. In a Finnish sample of 527 AD cases (ADGEN) and 8,707 controls (see Material and Methods), the comparison of allele number between AD patients (2 carriers) and controls (3 carriers) indicated overrepresentation of LoF variants in AD cases (OR = 11.0, 95% CI = 1.8-66.3; Pearson's χ^2 test, p = 0.0009; Fisher's exact test, p=0.03). In the ADES dataset (including 8,732 AD cases and 8,955 controls from Germany, France, Spain, the Netherlands and the United Kingdom (*7*)), the comparison of LoF allele number between AD patient (9 carriers) and control (one carrier) groups also indicated an overrepresentation in AD cases (OR = 9.2, 95% CI = 1.2-72.9; Pearson's χ^2 test, p = 0.01; Fisher's exact test p=0.01). Finally, a meta-analysis was performed, which, in turn, indicated that the *PLCG2* LoF variants increase the risk of AD (OR = 9.7, 95% CI = 2.0-47.7; p=0.005; **Fig. 5a** and **Table S2** for a full description of the LoF variants).

Effects of *PLCG2* LoF variants on AD pathological markers of AD and on *PLCG2* expression

We next analyzed the post-mortem sample obtained from the temporal cortex of an AD patient carrying the *PLCG2* LoF p.R953X variant to see whether partial loss-of-function of PLCγ2 influences AD-related neuropathology. This female was previously diagnosed as clinical AD and was classified as a Braak stage VI case according to neurofibrillary pathology in the neuropathological examination. Quantification of AD-related pathological hallmarks in the brain and CSF of this patient did not show any major alterations with respect to the Braak stage-matched AD patient samples (**Table S3** and **Fig. S6)**. The protein levels of PLCγ2 in brain lysates from the p.R953X carrier and four matched post-mortem AD samples were compared. As expected, protein levels of PLCγ2 were low in the cortical lysates based on Western blot analysis and a large variation was observed between individuals. However, protein levels of PLCγ2 were on average 70% lower in the *PLCG2* p.R953X variant carrier as compared to other AD cases (**Fig. 5b, c**). We did not detect additional specific bands for the p.R953X variant below the full-length PLCγ2. In addition, we had access to RNA extracted from the frozen blood sample of an ADGEN AD patient carrying the PLCG2 p.Q816X variant. We randomly selected four age-matched AD patients without *PLCG2* LoF variants from the ADGEN cohort. RNA analysis of these

samples revealed on average 40% reduction in the mRNA levels of *PLCG2* in the p.Q816X variant sample as compared to the other AD samples (**Fig. 5d**). However, the detailed examination of the RNA reads showed that the T allele (*i.e.*, allele encoding the stop codon)-containing reads were not completely excluded by nonsense-mediated mRNA decay (NMD) machinery as 20% of the total *PLCG2* reads still contained this allele. In conclusion, our data suggest that both LoF variants, *PLCG2* p.Q816X and *PLCG2* p.R953X, likely lead to NMD and therefore, reduce mRNA and protein levels of *PLCG2*/PLCγ2. However, we cannot rule out the possibility that low levels of truncated PLCγ2 are also produced.

Rescuing expression of *PLCG2* abolishes disease-related hallmarks in shPLCG2-hNCs

As NMD results in a decrease in the levels of PLCγ2, our shPLCG2-hNC model is relevant to assess the potential impact of the LoF variants on *PLCG2* expression and the subsequent phenotypes of interest. To confirm that the effect of *PLCG2* downregulation on AD hallmarks was specific, we performed rescue experiments by overexpressing *PLCG2* in shPLCG2-hNCs. Remarkably, restoring PLCγ2 levels also restored the full-length APP levels (**Fig. 5e, f**), Aβ levels (**Fig. 5g**), as well as total Tau levels (**Fig. 5e, f**) and Tau phosphorylation (**Fig. 5e, h**) close to shNT-hNCs levels. In addition, whereas downregulation of *PLCG2* was associated with a missorting of phosphorylated Tau into the soma, this pattern was largely abolished after *PLCG2* overexpression in shPLCG2-hNCs (**fig. 5i, j**). Finally, the observed changes in GSK3β and AKT phosphorylation levels were also restored after overexpressing *PLCG2* in shPLCG2-hNCs (**Fig. 5e, k**). In conclusion, restoring *PLCG2* expression in a human cellular model that mimics the consequences of *PLCG2* LoF on PLCγ2 levels can reverse the AD hallmark changes.

DISCUSSION

To determine if and how AD genetic risk factors contribute to synaptic failure, we developed an HCS to systematically characterize the impact of the downregulation of GWAS-defined genes on synaptic density. Surprisingly, among the genes with the strongest impact on synaptic density, *PLCG2* was one of the best hits (despite the absence of microglia in our HCS). This result was unexpected since in AD, *PLCG2* has been mostly studied in microglia and shown to be implicated in multiple microglia-related signaling pathways (*18–21*). However, strong evidence supports a role for PLCγ2 in synaptic function: (i) we and others found that *PLCG2* is also expressed in neurons (*23*, *25*); (ii) we observed that Plcγ2 is localized to both the pre- and post-synaptic compartments; (iii) we demonstrated that PLCγ2 downregulation impacts synaptic density and neuronal electrophysiological properties using three distinct experimental models (and different shRNAs). It is worth noting that downregulation of Plcγ2 *in vivo*, which leads to profound changes in DG granule cell morphology and physiology, was performed in adult (>3 months old) mice, thus precluding a potential developmental effect that could be argued to explain part of the synaptic phenotype observed in rat PNCs and hNCs.

Remarkably, we also observed that *PLCG2* downregulation in hNCs increases Tau phosphorylation as well as Aβ levels, suggesting that PLCγ2 participates in the development of the two main hallmarks of AD. Interestingly, our results highlight the AKT/GSK3β pathway, among others, to be involved in the neuronal response downstream of PLCγ2 downregulation. Indeed, a decrease in AKT activity and the subsequent increase in GSK3β activity has been previously described (*28*). GSK3β has already been shown to be involved in the regulation of the APP metabolism, Tau phosphorylation and synaptic functions (*29–31*), making it a credible intermediary between PLCγ2 and the different phenotypes associated with its downregulation. Of note, activation of the AKT/GSK3β pathway and increases in Aβ

levels/Tau phosphorylation were fully abolished when PLCγ2 level was restored, indicating a specific impact of PLCγ2 on these phenotypes. Interestingly, neurons derived from iPSCs obtained from sporadic AD cases also exhibit elevated Tau hyperphosphorylation, increased Aβ levels, and GSK3β activation (*32*).

To further support the importance of PLCγ2 and its downregulation in AD pathophysiology, we determined that rare LoF variants in *PLCG2* are associated with an increased risk of AD in two independent WES datasets. Two of these LoF variants, p.Q816X and p.R953X likely lead to NMD mechanisms resulting in decreased *PLCG2*/PLCγ2 expression. Our shPLCG2-hNC model is thus able to mimic the potential impact of these two LoF variants on *PLCG2* expression and consequently on AD phenotypes. In addition, at the genetic level, the association of LoF variants of *PLCG2* with increased AD risk is consistent with the fact that the functionally hypermorphic *PLCG2* p.P522R variant is protective against AD (*25*). In other words, an increase in the expression/activity of *PLCG2*/PLCγ2 is protective and a decrease is harmful. More specifically, the amino acid substitution P522R increases the activity of PLCγ2, which in turn enhances the conversion of phosphatidylinositol 4,5-bisphosphate (PIP2) to generate cytosolic inositol 3,4,5-trisphosphate (IP3) and diacylglycerol (DAG) (*18*, *20*, *33*). Thus, the enhanced activity of PLCγ2 may affect the generation of phosphatidylinositol 3,4,5-trisphosphate (PIP3) from PIP2 due to reduced substrate availability for phosphoinositide 3-kinase. This is important since PIP3 serves as a second messenger to recruit AKT and protein kinase C (PKC) to the plasma membrane, while the DAG-mediated activation of PKC can enhance AKT signaling through various mechanisms. This suggests that the observed alterations in the activity of AKT/GSK3β pathway in hNCs could be linked to the reduced total activity of PLCγ2. In this context, however, it should be noted that activity-related phosphorylation of Akt1/2 was significantly reduced in the brain tissue of Plcγ2-P522R knock-in (KI) mice (*18*), which is similar to what we observed in hNCs upon downregulation of PLCγ2. Finally, a previous study using human iPSC-derived microglia knockout for *PLCG2* and *TREM2* revealed a shared expressional dysregulation in these cells, emphasizing the importance of having sufficient levels and activity of PLCγ2 to avoid adverse cellular effects linked to AD (*34*). Although the focus in these previous studies has been set on microglia and myeloid-derived cells, a recent study using the cross-bred 5xFAD x Plcγ2-P522R KI mice revealed that the hypermorphic P522R variant improves impaired synaptic function as well as behavioral deficits observed in 5xFAD mice (*21*). This is particularly important in the context of the present study as the synaptic density and function were impaired in hNCs upon downregulation of PLCγ2. Collectively, these findings suggest a mechanism where the sustained activity of PLCγ2 becomes instrumental when the risk of AD (protective *vs* deleterious) is considered not only in microglia, but also in neurons.

In conclusion, our results report a new role for the AD genetic risk factor *PLCG2*. Downregulation of *PLCG2* specifically in neurons results in a signaling cascade leading to activation of GSK3β. This likely promotes increases in Aβ secretion, Tau hyperphosphorylation and synaptic dysfunction. This is in line with the observation that PLCγ2 may modulate Tau pathology and disease progression in patients with mild cognitive impairment (*35*). Emerging as a major genetic risk factor for AD (but also for other neurodegenerative diseases (*36*), *PLCG2* appears as a target of interest for drug development. In this context, determining which signaling pathways are related to *PLCG2,* not only in microglia, but also in neurons, will be important for identifying relevant druggable targets.

REFERENCES

1. C. Van Dyck, Lecanemab in Early Alzheimer's disease. *N Engl J Med.* **388**, 9-21 (2023).
2. K. Herrup, The case for rejecting the amyloid cascade hypothesis. *Nat. Neurosci.* **18**, 794–799 (2015).
3. D. J. Selkoe, J. Hardy, The amyloid hypothesis of Alzheimer's disease at 25 years. *EMBO Mol. Med.* **8**, 595–608 (2016).
4. G. B. Frisoni, D. Altomare, D. R. Thal, F. Ribaldi, R. van der Kant, R. Ossenkoppele, K. Blennow, J. Cummings, C. van Duijn, P. M. Nilsson, P. Y. Dietrich, P. Scheltens, B. Dubois, The probabilistic model of Alzheimer disease: the amyloid hypothesis revised. *Nat. Rev. Neurosci.* **23**, 53–66 (2022).
5. M. Gatz, C. A. Reynolds, L. Fratiglioni, B. Johansson, J. A. Mortimer, S. Berg, A. Fiske, N. L. Pedersen, Role of genes and environments for explaining Alzheimer disease. *Arch. Gen. Psychiatry* **63**, 168–174 (2006).
6. C. Bellenguez, F. Küçükali, I. E. Jansen, L. Kleineidam, S. Moreno-Grau, N. Amin, A. C. Naj, R. Campos-Martin, B. Grenier-Boley, V. Andrade, P. A. Holmans, A. Boland, V. Damotte, S. J. van der Lee, M. R. Costa, T. Kuulasmaa, Q. Yang, I. de Rojas, J. C. Bis, A. Yaqub, I. Prokic, J. Chapuis, S. Ahmad, V. Giedraitis, D. Aarsland, P. Garcia-Gonzalez, C. Abdelnour, E. Alarcón-Martín, D. Alcolea, M. Alegret, I. Alvarez, V. Álvarez, N. J. Armstrong, A. Tsolaki, C. Antúnez, I. Appollonio, M. Arcaro, S. Archetti, A. A. Pastor, B. Arosio, L. Athanasiu, H. Bailly, N. Banaj, M. Baquero, S. Barral, A. Beiser, A. B. Pastor, J. E. Below, P. Benchek, L. Benussi, C. Berr, C. Besse, V. Bessi, G. Binetti, A. Bizarro, R. Blesa, M. Boada, E. Boerwinkle, B. Borroni, S. Boschi, P. Bossù, G. Bråthen, J. Bressler, C. Bresner, H. Brodaty, K. J. Brookes, L. I. Brusco, D. Buiza-Rueda, K. Bûrger, V. Burholt, W. S. Bush, M. Calero, L. B. Cantwell, G. Chene, J. Chung, M. L. Cuccaro, Á. Carracedo, R. Cecchetti, L. Cervera-Carles, C. Charbonnier, H. H. Chen, C. Chillotti, S. Ciccone, J. A. H. R. Claassen, C. Clark, E. Conti, A. Corma-Gómez, E. Costantini, C. Custodero, D. Daian, M. C. Dalmasso, A. Daniele, E. Dardiotis, J. F. Dartigues, P. P. de Deyn, K. de Paiva Lopes, L. D. de Witte, S. Debette, J. Deckert, T. del Ser, N. Denning, A. DeStefano, M. Dichgans, J. Diehl-Schmid, M. Diez-Fairen, P. D. Rossi, S. Djurovic, E. Duron, E. Düzel, C. Dufouil, G. Eiriksdottir, S. Engelborghs, V. Escott-Price, A. Espinosa, M. Ewers, K. M. Faber, T. Fabrizio, S. F. Nielsen, D. W. Fardo, L. Farotti, C. Fenoglio, M. Fernández-Fuertes, R. Ferrari, C. B. Ferreira, E. Ferri, B. Fin, P. Fischer, T. Fladby, K. Fließbach, B. Fongang, M. Fornage, J. Fortea, T. M. Foroud, S. Fostinelli, N. C. Fox, E. Franco-Macías, M. J. Bullido, A. Frank-García, L. Froelich, B. Fulton-Howard, D. Galimberti, J. M. García-Alberca, P. García-González, S. Garcia-Madrona, G. Garcia-Ribas, R. Ghidoni, I. Giegling, G. Giorgio, A. M. Goate, O. Goldhardt, D. Gomez-Fonseca, A. González-Pérez, C. Graff, G. Grande, E. Green, T. Grimmer, E. Grünblatt, M. Grunin, V. Gudnason, T. Guetta-Baranes, A. Haapasalo, G. Hadjigeorgiou, J. L. Haines, K. L. Hamilton-Nelson, H. Hampel, O. Hanon, J. Hardy, A. M. Hartmann, L. Hausner, J. Harwood, S. Heilmann-Heimbach, S. Helisalmi, M. T. Heneka, I. Hernández, M. J. Herrmann, P. Hoffmann, C. Holmes, H. Holstege, R. H. Vilas, M. Hulsman, J. Humphrey, G. J. Biessels, X. Jian, C. Johansson, G. R. Jun, Y. Kastumata, J. Kauwe, P. G. Kehoe, L. Kilander, A. K. Ståhlbom, M. Kivipelto, A. Koivisto, J. Kornhuber, M. H. Kosmidis, W. A. Kukull, P. P. Kuksa, B. W. Kunkle, A. B. Kuzma, C. Lage, E. J. Laukka, L. Launer, A. Lauria, C. Y. Lee, J. Lehtisalo, O. Lerch, A. Lleó, W. Longstreth, O. Lopez, A. L. de Munain, S. Love, M. Löwemark, L. Luckcuck, K. L. Lunetta, Y. Ma, J. Macías, C. A. MacLeod, W. Maier, F. Mangialasche, M. Spallazzi, M. Marquié, R. Marshall, E. R. Martin, A. M. Montes, C. M. Rodríguez, C. Masullo, R. Mayeux, S. Mead, P. Mecocci, M. Medina, A. Meggy, S. Mehrabian, S. Mendoza, M. Menéndez-González, P. Mir, S. Moebus, M. Mol, L. Molina-Porcel, L. Montrreal, L. Morelli, F. Moreno, K. Morgan, T. Mosley, M. M. Nöthen, C. Muchnik, S. Mukherjee, B. Nacmias, T. Ngandu, G. Nicolas, B. G. Nordestgaard, R. Olaso, A. Orellana, M. Orsini, G. Ortega, A. Padovani, C. Paolo, G. Papenberg, L. Parnetti, F. Pasquier, P. Pastor, G. Peloso, A. Pérez-Cordón, J. Pérez-Tur, P. Pericard, O. Peters, Y. A. L. Pijnenburg, J. A. Pineda, G. Piñol-Ripoll, C. Pisanu, T. Polak, J. Popp, D. Posthuma, J.

Priller, R. Puerta, O. Quenez, I. Quintela, J. Q. Thomassen, A. Rábano, I. Rainero, F. Rajabli, I. Ramakers, L. M. Real, M. J. T. Reinders, C. Reitz, D. Reyes-Dumeyer, P. Ridge, S. Riedel-Heller, P. Riederer, N. Roberto, E. Rodriguez-Rodriguez, A. Rongve, I. R. Allende, M. Rosende-Roca, J. L. Royo, E. Rubino, D. Rujescu, M. E. Sáez, P. Sakka, I. Saltvedt, Á. Sanabria, M. B. Sánchez-Arjona, F. Sanchez-Garcia, P. S. Juan, R. Sánchez-Valle, S. B. Sando, C. Sarnowski, C. L. Satizabal, M. Scamosci, N. Scarmeas, E. Scarpini, P. Scheltens, N. Scherbaum, M. Scherer, M. Schmid, A. Schneider, J. M. Schott, G. Selbæk, D. Seripa, M. Serrano, J. Sha, A. A. Shadrin, O. Skrobot, S. Slifer, G. J. L. Snijders, H. Soininen, V. Solfrizzi, A. Solomon, Y. Song, S. Sorbi, O. Sotolongo-Grau, G. Spalletta, A. Spottke, A. Squassina, E. Stordal, J. P. Tartan, L. Tárraga, N. Tesí, A. Thalamuthu, T. Thomas, G. Tosto, L. Traykov, L. Tremolizzo, A. Tybjærg-Hansen, A. Uitterlinden, A. Ullgren, I. Ulstein, S. Valero, O. Valladares, C. Van Broeckhoven, J. Vance, B. N. Vardarajan, A. van der Lugt, J. Van Dongen, J. van Rooij, J. van Swieten, R. Vandenberghe, F. Verhey, J. S. Vidal, J. Vogelgsang, M. Vyhnalek, M. Wagner, D. Wallon, L. S. Wang, R. Wang, L. Weinhold, J. Wiltfang, G. Windle, B. Woods, M. Yannakoulia, H. Zare, Y. Zhao, X. Zhang, C. Zhu, M. Zulaica, J. Laczo, V. Matoska, M. Serpente, F. Assogna, F. Piras, F. Piras, V. Ciullo, J. Shofany, C. Ferrarese, S. Andreoni, G. Sala, C. P. Zoia, M. Del Zompo, A. Benussi, P. Bastiani, M. Takalo, T. Natunen, T. Laatikainen, J. Tuomilehto, R. Antikainen, T. Strandberg, J. Lindström, M. Peltonen, R. Abraham, A. Al-Chalabi, N. J. Bass, C. Brayne, K. S. Brown, J. Collinge, D. Craig, P. Deloukas, N. Fox, A. Gerrish, M. Gill, R. Gwilliam, D. Harold, P. Hollingworth, J. A. Johnston, L. Jones, B. Lawlor, G. Livingston, S. Lovestone, M. Lupton, A. Lynch, D. Mann, B. McGuinness, A. McQuillin, M. C. O'Donovan, M. J. Owen, P. Passmore, J. F. Powell, P. Proitsi, M. Rossor, C. E. Shaw, A. D. Smith, H. Gurling, S. Todd, C. Mummery, N. Ryan, G. Lacidogna, A. Adarmes-Gómez, A. Mauleón, A. Pancho, A. Gailhajenet, A. Lafuente, D. Macias-García, E. Martín, E. Pelejà, F. Carrillo, I. S. Merlín, L. Garrote-Espina, L. Vargas, M. Carrion-Claro, M. Marín, M. Labrador, M. Buendia, M. D. Alonso, M. Guitart, M. Moreno, M. Ibarria, M. Periñán, N. Aguilera, P. Gómez-Garre, P. Cañabate, R. Escuela, R. Pineda-Sánchez, R. Vigo-Ortega, S. Jesús, S. Preckler, S. Rodrigo-Herrero, S. Diego, A. Vacca, F. Roveta, N. Salvadori, E. Chipi, H. Boecker, C. Laske, R. Perneczky, C. Anastasiou, D. Janowitz, R. Malik, A. Anastasiou, K. Parveen, C. Lage, S. López-García, A. Antonell, K. Y. Mihova, D. Belezhanska, H. Weber, S. Kochen, P. Solis, N. Medel, J. Lisso, Z. Sevillano, D. G. Politis, V. Cores, C. Cuesta, C. Ortiz, J. I. Bacha, M. Rios, A. Saenz, M. S. Abalos, E. Kohler, D. L. Palacio, I. Etchepareborda, M. Kohler, G. Novack, F. A. Prestia, P. Galeano, E. M. Castaño, S. Germani, C. R. Toso, M. Rojo, C. Ingino, C. Mangone, D. C. Rubinsztein, S. Teipel, N. Fievet, V. Deramerourt, C. Forsell, H. Thonberg, M. Bjerke, E. De Roeck, M. T. Martínez-Larrad, N. Olivar, N. Aguilera, A. Cano, P. Cañabate, J. Macias, O. Maroñas, R. Nuñez-Llaves, C. Olivé, E. Pelejá, A. D. Adarmes-Gómez, M. D. Alonso, G. Amer-Ferrer, M. Antequera, J. A. Burguera, F. Carrillo, M. Carrión-Claro, M. J. Casajeros, M. Martinez de Pancorbo, R. Escuela, L. Garrote-Espina, P. Gómez-Garre, S. Hevilla, S. Jesús, M. A. L. Espinosa, A. Legaz, S. López-García, D. Macias-García, S. Manzanares, M. Marín, J. Marín-Muñoz, T. Marín, B. Martínez, V. Martínez, P. Martínez-Lage Álvarez, M. M. Iriarte, M. T. Periñán-Tocino, R. Pineda-Sánchez, D. Real de Asúa, S. Rodrigo, I. Sastre, M. P. Vicente, R. Vigo-Ortega, L. Vivancos, J. Epelbaum, D. Hannequin, D. campion, V. Deramecourt, C. Tzourio, A. Brice, B. Dubois, A. Williams, C. Thomas, C. Davies, W. Nash, K. Dowzell, A. C. Morales, M. Bernardo-Harrington, J. Turton, J. Lord, K. Brown, E. Vardy, E. Fisher, J. D. Warren, M. Rossor, N. S. Ryan, R. Guerreiro, J. Uphill, N. Bass, R. Heun, H. Kölsch, B. Schürmann, A. Lacour, C. Herold, J. A. Johnston, P. Passmore, J. Powell, Y. Patel, A. Hodges, T. Becker, D. Warden, G. Wilcock, R. Clarke, P. Deloukas, Y. Ben-Shlomo, N. M. Hooper, S. Pickering-Brown, R. Sussams, N. Warner, A. Bayer, I. Heuser, D. Drichel, N. Klopp, M. Mayhaus, M. Riemenschneider, S. Pinchler, T. Feulner, W. Gu, H. van den Bussche, M. Hüll, L. Frölich, H. E. Wichmann, K. H. Jöckel, M. O'Donovan, M. Owen, S. Bahrami, I. Bosnes, P. Selnes, S. Bergh, A. Palotie, M. Daly, H. Jacob, A. Matakidou, H. Runz, S. John, R. Plenge, M. McCarthy, J. Hunkapiller, M. Ehm, D. Waterworth, C. Fox, A. Malarstig, K. Klinger, K. Call, T. Behrens, P. Loerch, T. Mäkelä, J. Kaprio, P. Virolainen, K. Pulkki, T. Kilpi, M. Perola, J. Partanen, A. Pitkäranta, R. Kaarteenaho, S. Vainio, M. Turpeinen, R. Serpi, T. Laitinen, J. Mäkelä, V. M. Kosma, U. Kujala,

O. Tuovila, M. Hendolin, R. Pakkanen, J. Waring, B. Riley-Gillis, J. Liu, S. Biswas, D. Diogo, C. Marshall, X. Hu, M. Gossel, R. Graham, B. Cummings, S. Ripatti, J. Schleutker, M. Arvas, O. Carpén, R. Hinttala, J. Kettunen, A. Mannermaa, J. Laukkanen, V. Julkunen, A. Remes, R. Kälviäinen, J. Peltola, P. Tienari, J. Rinne, A. Ziemann, J. Waring, S. Esmaeeli, N. Smaoui, A. Lehtonen, S. Eaton, S. Lahdenperä, J. van Adelsberg, J. Michon, G. Kerchner, N. Bowers, E. Teng, J. Eicher, V. Mehta, P. Gormley, K. Linden, C. Whelan, F. Xu, D. Pulford, M. Färkkilä, S. Pikkarainen, A. Jussila, T. Blomster, M. Kiviniemi, M. Voutilainen, B. Georgantas, G. Heap, F. Rahimov, K. Usiskin, T. Lu, D. Oh, K. Kalpala, M. Miller, L. McCarthy, K. Eklund, A. Palomäki, P. Isomäki, L. Pirilä, O. Kaipiainen-Seppänen, J. Huhtakangas, A. Lertratanakul, M. Hochfeld, N. Bing, J. E. Gordillo, N. Mars, M. Pelkonen, P. Kauppi, H. Kankaanranta, T. Harju, D. Close, S. Greenberg, H. Chen, J. Betts, S. Ghosh, V. Salomaa, T. Niiranen, M. Juonala, K. Metsärinne, M. Kähönen, J. Junttila, M. Laakso, J. Pihlajamäki, J. Sinisalo, M. R. Taskinen, T. Tuomi, B. Challis, A. Peterson, A. Chu, J. Parkkinen, A. Muslin, H. Joensuu, T. Meretoja, L. Aaltonen, J. Mattson, A. Auranen, P. Karihtala, S. Kauppila, P. Auvinen, K. Elenius, R. Popovic, J. Schutzman, A. Loboda, A. Chhibber, H. Lehtonen, S. McDonough, M. Crohns, D. Kulkarni, K. Kaarniranta, J. A. Turunen, T. Ollila, S. Seitsonen, H. Uusitalo, V. Aaltonen, H. Uusitalo-Järvinen, M. Luodonpää, N. Hautala, S. Loomis, E. Strauss, H. Chen, A. Podgornaia, J. Hoffman, K. Tasanen, L. Huilaja, K. Hannula-Jouppi, T. Salmi, S. Peltonen, L. Koulu, I. Harvima, Y. Wu, D. Choy, P. Pussinen, A. Salminen, T. Salo, D. Rice, P. Nieminen, U. Palotie, M. Siponen, L. Suominen, P. Mäntylä, U. Gursoy, V. Anttonen, K. Sipilä, J. W. Davis, D. Quarless, S. Petrovski, E. Wigmore, C. Y. Chen, P. Bronson, E. Tsai, Y. Huang, J. Maranville, E. Shaikho, E. Mohammed, S. Wadhawan, E. Kvikstad, M. Caliskan, D. Chang, T. Bhangale, S. Pendergrass, E. Holzinger, X. Chen, Å. Hedman, K. S. King, C. Wang, E. Xu, F. Auge, C. Chatelain, D. Rajpal, D. Liu, K. Call, T. he Xia, M. Brauer, M. Kurki, J. Karjalainen, A. Havulinna, A. Jalanko, P. Palta, P. della Briotta Parolo, W. Zhou, S. Lemmelä, M. Rivas, J. Harju, A. Lehisto, A. Ganna, V. Llorens, H. Laivuori, S. Rüeger, M. E. Niemi, T. Tukiainen, M. P. Reeve, H. Heyne, K. Palin, J. Garcia-Tabuenca, H. Siirtola, T. Kiiskinen, J. Lee, K. Tsuo, A. Elliott, K. Kristiansson, K. Hyvärinen, J. Ritari, M. Koskinen, K. Pylkäs, M. Kalaoja, M. Karjalainen, T. Mantere, E. Kangasniemi, S. Heikkinen, E. Laakkonen, C. Sipeky, S. Heron, A. Karlsson, D. Jambulingam, V. S. Rathinakannan, R. Kajanne, M. Aavikko, M. G. Jiménez, P. della Briotta Parola, A. Lehistö, M. Kanai, M. Kaunisto, E. Kilpeläinen, T. P. Sipilä, G. Brein, G. Awaisa, A. Shcherban, K. Donner, A. Loukola, P. Laiho, T. Sistonen, E. Kaiharju, M. Laukkanen, E. Järvensivu, S. Lähteenmäki, L. Männikkö, R. Wong, H. Mattsson, T. Hiekkalinna, T. Paajanen, K. Pärn, J. Gracia-Tabuenca, E. Abner, P. M. Adams, A. Aguirre, M. S. Albert, R. L. Albin, M. Allen, L. Alvarez, L. G. Apostolova, S. E. Arnold, S. Asthana, C. S. Atwood, G. Ayres, C. T. Baldwin, R. C. Barber, L. L. Barnes, S. Barral, T. G. Beach, J. T. Becker, G. W. Beecham, D. Beekly, J. E. Below, P. Benchek, B. A. Benitez, D. Bennett, J. Bertelson, F. E. Margaret, T. D. Bird, D. Blacker, B. F. Boeve, J. D. Bowen, A. Boxer, J. Brewer, J. R. Burke, J. M. Burns, W. S. Bush, J. D. Buxbaum, N. J. Cairns, C. Cao, C. S. Carlson, C. M. Carlsson, R. M. Carney, M. M. Carrasquillo, S. Chasse, M. F. Chesselet, A. Chesi, N. A. Chin, H. C. Chui, J. Chung, S. Craft, P. K. Crane, D. H. Cribbs, E. A. Crocco, C. Cruchaga, M. Cullum, E. Darby, B. Davis, P. L. De Jager, C. DeCarli, J. DeToledo, M. Dick, D. W. Dickson, B. A. Dombroski, R. S. Doody, R. Duara, N. Ertekin-Taner, D. A. Evans, T. J. Fairchild, K. B. Fallon, M. R. Farlow, J. J. Farrell, V. Fernandez-Hernandez, S. Ferris, M. P. Frosch, B. Fulton-Howard, D. R. Galasko, A. Gamboa, M. Gearing, D. H. Geschwind, B. Ghetti, J. R. Gilbert, T. J. Grabowski, N. R. Graff-Radford, S. F. A. Grant, R. C. Green, J. H. Growdon, J. L. Haines, H. Hakonarson, J. Hall, R. L. Hamilton, O. Harari, L. E. Harrell, J. Haut, E. Head, V. W. Henderson, M. Hernandez, T. Hohman, L. S. Honig, R. M. Huebinger, M. J. Huentelman, C. M. Hulette, B. T. Hyman, L. S. Hynan, L. Ibanez, G. P. Jarvik, S. Jayadev, L. W. Jin, K. Johnson, L. Johnson, M. I. Kamboh, A. M. Karydas, M. J. Katz, J. A. Kaye, C. D. Keene, A. Khaleeq, R. Kim, J. Knebl, N. W. Kowall, J. H. Kramer, P. P. Kuksa, F. M. LaFerla, J. J. Lah, E. B. Larson, C. Y. Lee, E. B. Lee, A. Lerner, Y. Y. Leung, J. B. Leverenz, A. I. Levey, M. Li, A. P. Lieberman, R. B. Lipton, M. Logue, C. G. Lyketsos, J. Malamon, D. Mains, D. C. Marson, F. Martiniuk, D. C. Mash, E. Masliah, P. Massman, A. Masurkar, W. C. McCormick, S. M. McCurry, A. N. McDavid, S. McDonough, A. C. McKee, M.

Mesulam, J. Mez, B. L. Miller, C. A. Miller, J. W. Miller, T. J. Montine, E. S. Monuki, J. C. Morris, A. J. Myers, T. Nguyen, S. O'Bryant, J. M. Olichney, M. Ory, R. Palmer, J. E. Parisi, H. L. Paulson, V. Pavlik, D. Paydarfar, V. Perez, E. Peskind, R. C. Petersen, J. E. Phillips-Cremins, A. Pierce, M. Polk, W. W. Poon, H. Potter, L. Qu, M. Quiceno, J. F. Quinn, A. Raj, M. Raskind, E. M. Reiman, B. Reisberg, J. S. Reisch, J. M. Ringman, E. D. Roberson, M. Rodriguear, E. Rogaeva, H. J. Rosen, R. N. Rosenberg, D. R. Royall, M. A. Sager, M. Sano, A. J. Saykin, J. A. Schneider, L. S. Schneider, W. W. Seeley, S. H. Slifer, S. Small, A. G. Smith, J. P. Smith, Y. E. Song, J. A. Sonnen, S. Spina, P. S. George-Hyslop, R. A. Stern, A. B. Stevens, S. M. Strittmatter, D. Sultzer, R. H. Swerdlow, R. E. Tanzi, J. L. Tilson, J. Q. Trojanowski, J. C. Troncoso, D. W. Tsuang, O. Valladares, V. M. Van Deerlin, L. J. van Eldik, R. Vassar, H. V. Vinters, J. P. Vonsattel, S. Weintraub, K. A. Welsh-Bohmer, P. L. Whitehead, E. M. Wijsman, K. C. Wilhelmsen, B. Williams, J. Williamson, H. Wilms, T. S. Wingo, T. Wisniewski, R. L. Woltjer, M. Woon, C. B. Wright, C. K. Wu, S. G. Younkin, C. E. Yu, L. Yu, Y. Zhang, Y. Zhao, X. Zhu, H. Adams, R. O. Akinyemi, M. Ali, H. J. Aparicio, M. Bahadori, J. T. Becker, M. Breteler, D. Chasman, G. Chauhan, H. Comic, S. Cox, A. L. Cupples, G. Davies, C. S. DeCarli, M. G. Duperron, J. Dupuis, T. Evans, F. Fan, A. Fitzpatrick, A. E. Fohner, M. Ganguli, M. Geerlings, S. J. Glatt, H. M. Gonzalez, M. Goss, H. Grabe, M. Habes, S. R. Heckbert, E. Hofer, E. Hong, T. Hughes, T. F. Kautz, M. Knol, W. Kremen, P. Lacaze, J. Lahti, Q. Le Grand, E. Litkowski, S. Li, D. Liu, X. Liu, M. Loitfelder, A. Manning, P. Maillard, R. Marioni, B. Mazoyer, D. M. van Lent, H. Mei, A. Mishra, P. Nyquist, J. O'Connell, Y. Patel, T. Paus, Z. Pausova, K. Raikkonen-Talvitie, M. Riaz, S. Rich, J. Rotter, J. Romero, G. Roshchupkin, Y. Saba, M. Sargurupremraj, H. Schmidt, R. Schmidt, J. M. Shulman, J. Smith, H. Sekhar, R. Rajula, J. Shin, J. Simino, E. Sliz, A. Teumer, A. Thomas, A. Tin, E. Tucker-Drob, D. Vojinovic, Y. Wang, G. Weinstein, D. Williams, K. Wittfeld, L. Yanek, Y. Yang, L. A. Farrer, B. M. Psaty, M. Ghanbari, T. Raj, P. Sachdev, K. Mather, F. Jessen, M. A. Ikram, A. de Mendonça, J. Hort, M. Tsolaki, M. A. Pericak-Vance, P. Amouyel, J. Williams, R. Frikke-Schmidt, J. Clarimon, J. F. Deleuze, G. Rossi, S. Seshadri, O. A. Andreassen, M. Ingelsson, M. Hiltunen, K. Sleegers, G. D. Schellenberg, C. M. van Duijn, R. Sims, W. M. van der Flier, A. Ruiz, A. Ramirez, J. C. Lambert, New insights into the genetic etiology of Alzheimer's disease and related dementias. *Nat. Genet.* **54**, 412–436 (2022).

7. H. Holstege, M. Hulsman, C. Charbonnier, B. Grenier-Boley, O. Quenez, D. Grozeva, J. G. J. van Rooij, R. Sims, S. Ahmad, N. Amin, P. J. Norsworthy, O. Dols-Icardo, H. Hummerich, A. Kawalia, P. Amouyel, G. W. Beecham, C. Berr, J. C. Bis, A. Boland, P. Bossù, F. Bouwman, J. Bras, D. Campion, J. N. Cochran, A. Daniele, J. F. Dartigues, S. Debette, J. F. Deleuze, N. Denning, A. L. DeStefano, L. A. Farrer, M. V. Fernández, N. C. Fox, D. Galimberti, E. Genin, J. J. P. Gille, Y. Le Guen, R. Guerreiro, J. L. Haines, C. Holmes, M. A. Ikram, M. K. Ikram, I. E. Jansen, R. Kraaij, M. Lathrop, A. W. Lemstra, A. Lleó, L. Luckcuck, M. M. A. M. Mannens, R. Marshall, E. R. Martin, C. Masullo, R. Mayeux, P. Mecocci, A. Meggy, M. O. Mol, K. Morgan, R. M. Myers, B. Nacmias, A. C. Naj, V. Napolioni, F. Pasquier, P. Pastor, M. A. Pericak-Vance, R. Raybould, R. Redon, M. J. T. Reinders, A. C. Richard, S. G. Riedel-Heller, F. Rivadeneira, S. Rousseau, N. S. Ryan, S. Saad, P. Sanchez-Juan, G. D. Schellenberg, P. Scheltens, J. M. Schott, D. Seripa, S. Seshadri, D. Sie, E. A. Sistermans, S. Sorbi, R. van Spaendonk, G. Spalletta, N. Tesi, B. Tijms, A. G. Uitterlinden, S. J. van der Lee, P. J. Visser, M. Wagner, D. Wallon, L. S. Wang, A. Zarea, J. Clarimon, J. C. van Swieten, M. D. Greicius, J. S. Yokoyama, C. Cruchaga, J. Hardy, A. Ramirez, S. Mead, W. M. van der Flier, C. M. van Duijn, J. Williams, G. Nicolas, C. Bellenguez, J. C. Lambert, Exome sequencing identifies rare damaging variants in ATP8B4 and ABCA1 as risk factors for Alzheimer's disease. *Nat. Genet.* **54**, 1786–1794 (2022).
8. J. C. Lambert, A. Ramirez, B. Grenier-Boley, C. Bellenguez, Step by step: towards a better understanding of the genetic architecture of Alzheimer's disease. *Mol. Psychiatry.* **28**, 2716-2727 (2023).
9. B. Schürmann, D. P. Bermingham, K. J. Kopeikina, K. Myczek, S. Yoon, K. E. Horan, C. J. Kelly, M. D. Martin-de-Saavedra, M. P. Forrest, J. M. Fawcett-Patel, K. R. Smith, R. Gao, A. Bach, A. C. Burette, J. Z. Rappoport, R. J. Weinberg, M. Martina, P. Penzes, A novel role for the late-onset Alzheimer's disease (LOAD)-associated protein Bin1 in regulating postsynaptic trafficking and

glutamatergic signaling. *Mol. Psychiatry* **25**, 2000–2016 (2020).
10. F. Eysert, A. Coulon, E. Boscher, A. C. Vreulx, A. Flaig, T. Mendes, S. Hughes, B. Grenier-Boley, X. Hanoulle, F. Demiautte, C. Bauer, M. Marttinen, M. Takalo, P. Amouyel, S. Desai, I. Pike, M. Hiltunen, F. Chécler, M. Farinelli, C. Delay, N. Malmanche, S. S. Hébert, J. Dumont, D. Kilinc, J. C. Lambert, J. Chapuis, Alzheimer's genetic risk factor FERMT2 (Kindlin-2) controls axonal growth and synaptic plasticity in an APP-dependent manner. *Mol. Psychiatry* **26**, 5592–5607 (2021).
11. A. Giralt, V. Brito, Q. Chevy, C. Simonnet, Y. Otsu, C. Cifuentes-DÍaz, B. De Pins, R. Coura, J. Alberch, S. Ginés, J. C. Poncer, J. A. Girault, Pyk2 modulates hippocampal excitatory synapses and contributes to cognitive deficits in a Huntington's disease model. *Nat. Commun. 2017 81* **8**, 1–16 (2017).
12. S. A. Ojelade, T. V. Lee, N. Giagtzoglou, L. Yu, B. Ugur, Y. Li, L. Duraine, Z. Zuo, V. Petyuk, P. L. De Jager, D. A. Bennett, B. R. Arenkiel, H. J. Bellen, J. M. Shulman, cindr, the Drosophila Homolog of the CD2AP Alzheimer's Disease Risk Gene, Is Required for Synaptic Transmission and Proteostasis. *Cell Rep.* **28**, 1799-1813.e5 (2019).
13. E. Masliah, Mechanisms of synaptic dysfunction in Alzheimer's disease. *Histol. Histopathol.* **10**, 509-19 (1995).
14. G. Barthet, C. Mulle, Presynaptic failure in Alzheimer's disease. *Prog. Neurobiol.* **194**, 101801. (2020).
15. S. Ribarič, Detecting Early Cognitive Decline in Alzheimer's Disease with Brain Synaptic Structural and Functional Evaluation. *Biomedicines* **11**, 355 (2023).
16. A. Coulon, D. Siedlecki-Wullich, C. Najdek, C. Gelle, A. M. Ayral, F. Demiautte, E. Lambert, A. Vandeputte, P. Brodin, T. Mendes, J. C. Lambert, D. Kilinc, J. Dumont, J. Chapuis, High-Content Screening of Synaptic Density Modulators in Primary Neuronal Cultures. *Curr. Protoc.* **3** (2023).
17. D. Kilinc, A.-C. Vreulx, T. Mendes, A. Flaig, D. Marques-Coelho, M. Verschoore, F. Demiautte, P. Amouyel, F. Eysert, P. Dourlen, J. Chapuis, M. R. Costa, N. Malmanche, F. Checler, J.-C. Lambert, Pyk2 overexpression in postsynaptic neurons blocks amyloid β1-42-induced synaptotoxicity in microfluidic co-cultures. *Brain Commun.* **2,** fcaa139 (2020).
18. M. Takalo, R. Wittrahm, B. Wefers, S. Parhizkar, K. Jokivarsi, T. Kuulasmaa, P. Mäkinen, H. Martiskainen, W. Wurst, X. Xiang, M. Marttinen, P. Poutiainen, A. Haapasalo, M. Hiltunen, C. Haass, The Alzheimer's disease-associated protective Plcγ2-P522R variant promotes immune functions. *Mol. Neurodegener.* **15**, 1–14 (2020).
19. C. Claes, W. E. England, E. P. Danhash, S. Kiani Shabestari, A. Jairaman, J. P. Chadarevian, J. Hasselmann, A. P. Tsai, M. A. Coburn, J. Sanchez, T. E. Lim, J. L. S. Hidalgo, C. Tu, M. D. Cahalan, B. T. Lamb, G. E. Landreth, R. C. Spitale, M. Blurton-Jones, H. Davtyan, The P522R protective variant of PLCG2 promotes the expression of antigen presentation genes by human microglia in an Alzheimer's disease mouse model. *Alzheimers. Dement.* **18**, 1765-1778 (2022).
20. A. P. Tsai, C. Dong, P. B. C. Lin, E. J. Messenger, B. T. Casali, M. Moutinho, Y. Liu, A. L. Oblak, B. T. Lamb, G. E. Landreth, S. J. Bissel, K. Nho, PLCG2 is associated with the inflammatory response and is induced by amyloid plaques in Alzheimer's disease. *Genome Med.* **14**, 17 (2022).
21. A. P. Tsai, C. Dong, P. B. C. Lin, A. L. Oblak, G. Viana Di Prisco, N. Wang, N. Hajicek, A. J. Carr, E. K. Lendy, O. Hahn, M. Atkins, A. G. Foltz, J. Patel, G. Xu, M. Moutinho, J. Sondek, Q. Zhang, A. D. Mesecar, Y. Liu, B. K. Atwood, T. Wyss-Coray, K. Nho, S. J. Bissel, B. T. Lamb, G. E. Landreth, Genetic variants of phospholipase C-γ2 alter the phenotype and function of microglia and confer differential risk for Alzheimer's disease. *Immunity* **56**, 2121-2136.e6 (2023).
22. Z. Yao, C. T. J. van Velthoven, T. N. Nguyen, J. Goldy, A. E. Sedeno-Cortes, F. Baftizadeh, D. Bertagnolli, T. Casper, M. Chiang, K. Crichton, S. L. Ding, O. Fong, E. Garren, A. Glandon, N. W. Gouwens, J. Gray, L. T. Graybuck, M. J. Hawrylycz, D. Hirschstein, M. Kroll, K. Lathia, C. Lee, B. Levi, D. McMillen, S. Mok, T. Pham, Q. Ren, C. Rimorin, N. Shapovalova, J. Sulc, S. M. Sunkin, M. Tieu, A. Torkelson, H. Tung, K. Ward, N. Dee, K. A. Smith, B. Tasic, H. Zeng, A taxonomy of transcriptomic cell types across the isocortex and hippocampal formation. *Cell* **184**, 3222-3241.e26 (2021).

23. K. Leng, E. Li, R. Eser, A. Piergies, R. Sit, M. Tan, N. Neff, S. H. Li, R. D. Rodriguez, C. K. Suemoto, R. E. P. Leite, A. J. Ehrenberg, C. A. Pasqualucci, W. W. Seeley, S. Spina, H. Heinsen, L. T. Grinberg, M. Kampmann, Molecular characterization of selectively vulnerable neurons in Alzheimer's disease. *Nat. Neurosci.* **24**, 276–287 (2021).
24. O. Saha, A. R. Melo de Farias, A. Pelletier, D. Siedlecki-Wullich, B. S. Landeira, J. Gadaut, A. Carrier, A. C. Vreulx, K. Guyot, Y. Shen, A. Bonnefond, P. Amouyel, J. TCW, D. Kilinc, C. M. Queiroz, F. Delahaye, J. C. Lambert, M. R. Costa, The Alzheimer's disease risk gene BIN1 regulates activity-dependent gene expression in human-induced glutamatergic neurons. *Mol. Psychiatry*, doi: 10.1038/S41380-024-02502-Y (2024).
25. L. Magno, C. B. Lessard, M. Martins, V. Lang, P. Cruz, Y. Asi, M. Katan, J. Bilsland, T. Lashley, P. Chakrabarty, T. E. Golde, P. J. Whiting, Alzheimer's disease phospholipase C-gamma-2 (PLCG2) protective variant is a functional hypermorph. *Alzheimers. Res. Ther.* **11**, 16 (2019).
26. N. Jiang, D. Cupolillo, N. Grosjean, E. Muller, S. Deforges, C. Mulle, T. Amédée, Impaired plasticity of intrinsic excitability in the dentate gyrus alters spike transfer in a mouse model of Alzheimer's disease. *Neurobiol. Dis.* **154**, 105345 (2021)..
27. S. Viana Da Silva, P. Zhang, M. G. Haberl, V. Labrousse, N. Grosjean, C. Blanchet, A. Frick, C. Mulle, Hippocampal Mossy Fibers Synapses in CA3 Pyramidal Cells Are Altered at an Early Stage in a Mouse Model of Alzheimer's Disease. *J. Neurosci.* **39**, 4193–4205 (2019).
28. B. W. Doble, J. R. Woodgett, GSK-3: tricks of the trade for a multi-tasking kinase. *J. Cell Sci.* **116**, 1175–1186 (2003).
29. P. H. Reddy, Amyloid beta-induced glycogen synthase kinase 3β phosphorylated VDAC1 in Alzheimer's disease: implications for synaptic dysfunction and neuronal damage. *Biochim. Biophys. Acta* **1832**, 1913–1921 (2013).
30. F. Hernandez, J. J. Lucas, J. Avila, GSK3 and tau: two convergence points in Alzheimer's disease. *J. Alzheimers. Dis.* **33 Suppl 1** (2013).
31. P. T. T. Ly, Y. Wu, H. Zou, R. Wang, W. Zhou, A. Kinoshita, M. Zhang, Y. Yang, F. Cai, J. Woodgett, W. Song, Inhibition of GSK3β-mediated BACE1 expression reduces Alzheimer-associated phenotypes. *J. Clin. Invest.* **123**, 224–235 (2013).
32. A. Ochalek, B. Mihalik, H. X. Avci, A. Chandrasekaran, A. Téglási, I. Bock, M. Lo Giudice, Z. Táncos, K. Molnár, L. László, J. E. Nielsen, B. Holst, K. Freude, P. Hyttel, J. Kobolák, A. Dinnyés, Neurons derived from sporadic Alzheimer's disease iPSCs reveal elevated TAU hyperphosphorylation, increased amyloid levels, and GSK3B activation. *Alzheimers. Res. Ther.* **9**, 90 (2017).
33. S. Solomon, N. K. Sampathkumar, I. Carre, M. Mondal, G. Chennell, A. C. Vernon, M. D. Ruepp, J. C. Mitchell, Heterozygous expression of the Alzheimer's disease-protective PLCγ2 P522R variant enhances Aβ clearance while preserving synapses. *Cell. Mol. Life Sci.* **79**, 453 (2022).
34. B. J. Andreone, L. Przybyla, C. Llapashtica, A. Rana, S. S. Davis, B. van Lengerich, K. Lin, J. Shi, Y. Mei, G. Astarita, G. Di Paolo, T. Sandmann, K. M. Monroe, J. W. Lewcock, Alzheimer's-associated PLCγ2 is a signaling node required for both TREM2 function and the inflammatory response in human microglia. *Nat. Neurosci.* **23**, 927–938 (2020).
35. L. Kleineidam, V. Chouraki, T. Próchnicki, S. J. van der Lee, L. Madrid-Márquez, H. Wagner-Thelen, I. Karaca, L. Weinhold, S. Wolfsgruber, A. Boland, P. V. Martino Adami, P. Lewczuk, J. Popp, F. Brosseron, I. E. Jansen, M. Hulsman, J. Kornhuber, O. Peters, C. Berr, R. Heun, L. Frölich, C. Tzourio, J. F. Dartigues, M. Hüll, A. Espinosa, I. Hernández, I. de Rojas, A. Orellana, S. Valero, N. Stringa, N. M. van Schoor, M. Huisman, P. Scheltens, P. Amouyel, A. Ramirez, E. Rüther, J. F. Deleuze, J. Wiltfang, L. Tarraga, M. Schmid, M. Scherer, S. Riedel-Heller, M. T. Heneka, P. Amouyel, F. Jessen, M. Boada, W. Maier, A. Schneider, A. González-Pérez, W. M. van der Flier, M. Wagner, J. C. Lambert, H. Holstege, M. ªE Sáez, E. Latz, A. Ruiz, PLCG2 protective variant p.P522R modulates tau pathology and disease progression in patients with mild cognitive impairment. *Acta Neuropathol.* **139**, 1025–1044 (2020).
36. S. J. van der Lee, O. J. Conway, I. Jansen, M. M. Carrasquillo, L. Kleineidam, E. van den Akker, I. Hernández, K. R. van Eijk, N. Stringa, J. A. Chen, A. Zettergren, T. F. M. Andlauer, M. Diez-Fairen, J. Simon-Sanchez, A. Lleó, H. Zetterberg, M. Nygaard, C. Blauwendraat, J. E. Savage, J. Mengel-

From, S. Moreno-Grau, M. Wagner, J. Fortea, M. J. Keogh, K. Blennow, I. Skoog, M. A. Friese, O. Pletnikova, M. Zulaica, C. Lage, I. de Rojas, S. Riedel-Heller, I. Illán-Gala, W. Wei, B. Jeune, A. Orellana, F. Then Bergh, X. Wang, M. Hulsman, N. Beker, N. Tesi, C. M. Morris, B. Indakoetxea, L. E. Collij, M. Scherer, E. Morenas-Rodríguez, J. W. Ironside, B. N. M. van Berckel, D. Alcolea, H. Wiendl, S. L. Strickland, P. Pastor, E. Rodríguez Rodríguez, B. F. Boeve, R. C. Petersen, T. J. Ferman, J. A. van Gerpen, M. J. T. Reinders, R. J. Uitti, L. Tárraga, W. Maier, O. Dols-Icardo, A. Kawalia, M. C. Dalmasso, M. Boada, U. K. Zettl, N. M. van Schoor, M. Beekman, M. Allen, E. Masliah, A. L. de Munain, A. Pantelyat, Z. K. Wszolek, O. A. Ross, D. W. Dickson, N. R. Graff-Radford, D. Knopman, R. Rademakers, A. W. Lemstra, Y. A. L. Pijnenburg, P. Scheltens, T. Gasser, P. F. Chinnery, B. Hemmer, M. A. Huisman, J. Troncoso, F. Moreno, E. A. Nohr, T. I. A. Sørensen, P. Heutink, P. Sánchez-Juan, D. Posthuma, G. Coppola, A. M. Karydas, A. Varpetian, T. M. Foroud, A. I. Levey, W. A. Kukull, M. F. Mendez, J. Ringman, H. Chui, C. Cotman, C. DeCarli, B. L. Miller, D. H. Geschwind, J. Clarimón, K. Christensen, N. Ertekin-Taner, S. W. Scholz, A. Ramirez, A. Ruiz, E. Slagboom, W. M. van der Flier, H. Holstege, A nonsynonymous mutation in PLCG2 reduces the risk of Alzheimer's disease, dementia with Lewy bodies and frontotemporal dementia, and increases the likelihood of longevity. *Acta Neuropathol.* **138**, 237–250 (2019).

37. S. Kaech, G. Banker, Culturing hippocampal neurons. *Nat. Protoc.* **1**, 2406–2415 (2006).

38. B. W. Kunkle, B. Grenier-Boley, R. Sims, J. C. Bis, V. Damotte, A. C. Naj, A. Boland, M. Vronskaya, S. J. van der Lee, A. Amlie-Wolf, C. Bellenguez, A. Frizatti, V. Chouraki, E. R. Martin, K. Sleegers, N. Badarinarayan, J. Jakobsdottir, K. L. Hamilton-Nelson, S. Moreno-Grau, R. Olaso, R. Raybould, Y. Chen, A. B. Kuzma, M. Hiltunen, T. Morgan, S. Ahmad, B. N. Vardarajan, J. Epelbaum, P. Hoffmann, M. Boada, G. W. Beecham, J.-G. Garnier, D. Harold, A. L. Fitzpatrick, O. Valladares, M.-L. Moutet, A. Gerrish, A. V. Smith, L. Qu, D. Bacq, N. Denning, X. Jian, Y. Zhao, M. Del Zompo, N. C. Fox, S.-H. Choi, I. Mateo, J. T. Hughes, H. H. Adams, J. Malamon, F. Sanchez-Garcia, Y. Patel, J. a. Brody, B. a. Dombroski, M. C. D. Naranjo, M. Daniilidou, G. Eiriksdottir, S. Mukherjee, D. Wallon, J. Uphill, T. Aspelund, L. B. Cantwell, F. Garzia, D. Galimberti, E. Hofer, M. Butkiewicz, B. Fin, E. Scarpini, C. Sarnowski, W. S. Bush, S. Meslage, J. Kornhuber, C. C. White, Y. Song, R. C. Barber, S. Engelborghs, S. Sordon, D. Voijnovic, P. M. Adams, R. Vandenberghe, M. Mayhaus, L. A. Cupples, M. S. Albert, P. P. De Deyn, W. Gu, J. J. Himali, D. Beekly, A. Squassina, A. M. Hartmann, A. Orellana, D. Blacker, E. Rodriguez-Rodriguez, S. Lovestone, M. E. Garcia, R. S. Doody, C. Munoz-Fernadez, R. Sussams, H. Lin, T. J. Fairchild, Y. a. Benito, C. Holmes, H. Karamujić-Čomić, M. P. Frosch, H. Thonberg, W. Maier, G. Roschupkin, B. Ghetti, V. Giedraitis, A. Kawalia, S. Li, R. M. Huebinger, L. Kilander, S. Moebus, I. Hernández, M. I. Kamboh, R. Brundin, J. Turton, Q. Yang, M. J. Katz, L. Concari, J. Lord, A. S. Beiser, C. D. Keene, S. Helisalmi, I. Kloszewska, W. a. Kukull, A. M. Koivisto, A. Lynch, L. Tarraga, E. B. Larson, A. Haapasalo, B. Lawlor, T. H. Mosley, R. B. Lipton, V. Solfrizzi, M. Gill, W. T. Longstreth, T. J. Montine, V. Frisardi, M. Diez-Fairen, F. Rivadeneira, R. C. Petersen, V. Deramecourt, I. Alvarez, F. Salani, A. Ciaramella, E. Boerwinkle, E. M. Reiman, N. Fievet, J. I. Rotter, J. S. Reisch, O. Hanon, C. Cupidi, a. G. Andre Uitterlinden, D. R. Royall, C. Dufouil, R. G. Maletta, I. de Rojas, M. Sano, A. Brice, R. Cecchetti, P. S. George-Hyslop, K. Ritchie, M. Tsolaki, D. W. Tsuang, B. Dubois, D. Craig, C.-K. Wu, H. Soininen, D. Avramidou, R. L. Albin, L. Fratiglioni, A. Germanou, L. G. Apostolova, L. Keller, M. Koutroumani, S. E. Arnold, F. Panza, O. Gkatzima, S. Asthana, D. Hannequin, P. Whitehead, C. S. Atwood, P. Caffarra, H. Hampel, I. Quintela, Á. Carracedo, L. Lannfelt, D. C. Rubinsztein, L. L. Barnes, F. Pasquier, L. Frölich, S. Barral, B. McGuinness, T. G. Beach, J. a. Johnston, J. T. Becker, P. Passmore, E. H. Bigio, J. M. Schott, T. D. Bird, J. D. Warren, B. F. Boeve, M. K. Lupton, J. D. Bowen, P. Proitsi, A. Boxer, J. F. Powell, J. R. Burke, J. S. K. Kauwe, J. M. Burns, M. Mancuso, J. D. Buxbaum, U. Bonuccelli, N. J. Cairns, A. McQuillin, C. Cao, G. Livingston, C. S. Carlson, N. J. Bass, C. M. Carlsson, J. Hardy, R. M. Carney, J. Bras, M. M. Carrasquillo, R. Guerreiro, M. Allen, H. C. Chui, E. Fisher, C. Masullo, E. a. Crocco, C. DeCarli, G. Bisceglio, M. Dick, L. Ma, R. Duara, N. R. Graff-Radford, D. a. Evans, A. Hodges, K. M. Faber, M. Scherer, K. B. Fallon, M. Riemenschneider, D. W. Fardo, R. Heun, M. R. Farlow, H. Kölsch, S. Ferris, M. Leber, T. M. Foroud, I. Heuser, D. R. Galasko, I. Giegling, M. Gearing, M. Hüll, D. H. Geschwind, J. R.

Gilbert, J. Morris, R. C. Green, K. Mayo, J. H. Growdon, T. Feulner, R. L. Hamilton, L. E. Harrell, D. Drichel, L. S. Honig, T. D. Cushion, M. J. Huentelman, P. Hollingworth, C. M. Hulette, B. T. Hyman, R. Marshall, G. P. Jarvik, A. Meggy, E. Abner, G. E. Menzies, L.-W. Jin, G. Leonenko, L. M. Real, G. R. Jun, C. T. Baldwin, D. Grozeva, A. Karydas, G. Russo, J. a. Kaye, R. Kim, F. Jessen, N. W. Kowall, B. Vellas, J. H. Kramer, E. Vardy, F. M. LaFerla, K.-H. Jöckel, J. J. Lah, M. Dichgans, J. B. Leverenz, D. Mann, A. I. Levey, S. Pickering-Brown, A. P. Lieberman, N. Klopp, K. L. Lunetta, H.-E. Wichmann, C. G. Lyketsos, K. Morgan, D. C. Marson, K. Brown, F. Martiniuk, C. Medway, D. C. Mash, M. M. Nöthen, E. Masliah, N. M. Hooper, W. C. McCormick, A. Daniele, S. M. McCurry, A. Bayer, A. N. McDavid, J. Gallacher, A. C. McKee, H. van den Bussche, M. Mesulam, C. Brayne, B. L. Miller, S. Riedel-Heller, C. a. Miller, J. W. Miller, A. Al-Chalabi, J. C. Morris, C. E. Shaw, A. J. Myers, J. Wiltfang, S. O'Bryant, J. M. Olichney, V. Alvarez, J. E. Parisi, A. B. Singleton, H. L. Paulson, J. Collinge, W. R. Perry, S. Mead, E. Peskind, D. H. Cribbs, M. Rossor, A. Pierce, N. S. Ryan, W. W. Poon, B. Nacmias, H. Potter, S. Sorbi, J. F. Quinn, E. Sacchinelli, A. Raj, G. Spalletta, M. Raskind, C. Caltagirone, P. Bossù, M. D. Orfei, B. Reisberg, R. Clarke, C. Reitz, a D. Smith, J. M. Ringman, D. Warden, E. D. Roberson, G. Wilcock, E. Rogaeva, A. C. Bruni, H. J. Rosen, M. Gallo, R. N. Rosenberg, Y. Ben-Shlomo, M. a. Sager, P. Mecocci, A. J. Saykin, P. Pastor, M. L. Cuccaro, J. M. Vance, J. a. Schneider, L. S. Schneider, S. Slifer, W. W. Seeley, A. G. Smith, J. a. Sonnen, S. Spina, R. a. Stern, R. H. Swerdlow, M. Tang, R. E. Tanzi, J. Q. Trojanowski, J. C. Troncoso, V. M. Van Deerlin, L. J. Van Eldik, H. V. Vinters, J. P. Vonsattel, S. Weintraub, K. a. Welsh-Bohmer, K. C. Wilhelmsen, J. Williamson, T. S. Wingo, R. L. Woltjer, C. B. Wright, C.-E. Yu, L. Yu, Y. Saba, A. Pilotto, M. J. Bullido, O. Peters, P. K. Crane, D. Bennett, P. Bosco, E. Coto, V. Boccardi, P. L. De Jager, A. Lleo, N. Warner, O. L. Lopez, M. Ingelsson, P. Deloukas, C. Cruchaga, C. Graff, R. Gwilliam, M. Fornage, A. M. Goate, P. Sanchez-Juan, P. G. Kehoe, N. Amin, N. Ertekin-Taner, C. Berr, S. Debette, S. Love, L. J. Launer, S. G. Younkin, J.-F. Dartigues, C. Corcoran, M. A. Ikram, D. W. Dickson, G. Nicolas, D. Campion, J. Tschanz, H. Schmidt, H. Hakonarson, J. Clarimon, R. Munger, R. Schmidt, L. a. Farrer, C. Van Broeckhoven, M. C. O'Donovan, A. L. DeStefano, L. Jones, J. L. Haines, J.-F. Deleuze, M. J. Owen, V. Gudnason, R. Mayeux, V. Escott-Price, B. M. Psaty, A. Ramirez, L.-S. Wang, A. Ruiz, C. M. van Duijn, P. a. Holmans, S. Seshadri, J. Williams, P. Amouyel, G. D. Schellenberg, J.-C. Lambert, M. a. Pericak-Vance, Genetic meta-analysis of diagnosed Alzheimer's disease identifies new risk loci and implicates Aβ, tau, immunity and lipid processing. *Nat. Genet.* **51**, 414–430 (2019).

39. A. Blasiak, G. U. Lee, D. Kilinc, Neuron Subpopulations with Different Elongation Rates and DCC Dynamics Exhibit Distinct Responses to Isolated Netrin-1 Treatment. *ACS Chem. Neurosci.* **6**, 1578–1590 (2015).
40. A. Rodriguez, D. B. Ehlenberger, P. R. Hof, S. L. Wearne, Rayburst sampling, an algorithm for automated three-dimensional shape analysis from laser scanning microscopy images. *Nat. Protoc.* **1**, 2152–61 (2006).
41. J. Schindelin, I. Arganda-Carreras, E. Frise, V. Kaynig, M. Longair, T. Pietzsch, S. Preibisch, C. Rueden, S. Saalfeld, B. Schmid, J.-Y. Tinevez, D. J. White, V. Hartenstein, K. Eliceiri, P. Tomancak, A. Cardona, Fiji: an open-source platform for biological-image analysis. *Nat. Methods* **9**, 676–82 (2012).
42. G. McKhann, D. Drachman, M. Folstein, R. Katzman, D. Price, E. M. Stadlan, Clinical diagnosis of Alzheimer's disease: report of the NINCDS-ADRDA Work Group under the auspices of Department of Health and Human Services Task Force on Alzheimer's Disease. *Neurology* **34**, 939–944 (1984).
43. J. C. Bis, X. Jian, B. W. Kunkle, Y. Chen, K. L. Hamilton-Nelson, W. S. Bush, W. J. Salerno, D. Lancour, Y. Ma, A. E. Renton, E. Marcora, J. J. Farrell, Y. Zhao, L. Qu, S. Ahmad, N. Amin, P. Amouyel, G. W. Beecham, J. E. Below, D. Campion, L. Cantwell, C. Charbonnier, J. Chung, P. K. Crane, C. Cruchaga, L. A. Cupples, J. F. Dartigues, S. Debette, J. F. Deleuze, L. Fulton, S. B. Gabriel, E. Genin, R. A. Gibbs, A. Goate, B. Grenier-Boley, N. Gupta, J. L. Haines, A. S. Havulinna, S. Helisalmi, M. Hiltunen, D. P. Howrigan, M. A. Ikram, J. Kaprio, J. Konrad, A. Kuzma, E. S. Lander, M. Lathrop, T. Lehtimäki, H. Lin, K. Mattila, R. Mayeux, D. M. Muzny, W. Nasser, B. Neale, K.

Nho, G. Nicolas, D. Patel, M. A. Pericak-Vance, M. Perola, B. M. Psaty, O. Quenez, F. Rajabli, R. Redon, C. Reitz, A. M. Remes, V. Salomaa, C. Sarnowski, H. Schmidt, M. Schmidt, R. Schmidt, H. Soininen, T. A. Thornton, G. Tosto, C. Tzourio, S. J. van der Lee, C. M. van Duijn, O. Valladares, B. Vardarajan, L. S. Wang, W. Wang, E. Wijsman, R. K. Wilson, D. Witten, K. C. Worley, X. Zhang, C. Bellenguez, J. C. Lambert, M. I. Kurki, A. Palotie, M. Daly, E. Boerwinkle, K. L. Lunetta, A. L. Destefano, J. Dupuis, E. R. Martin, G. D. Schellenberg, S. Seshadri, A. C. Naj, M. Fornage, L. A. Farrer, Whole exome sequencing study identifies novel rare and common Alzheimer's-Associated variants involved in immune response and transcriptional regulation. *Mol. Psychiatry* **25**, 1859–1875 (2020).

44. A. Korpioja, J. Krüger, S. Koivuluoma, K. Pylkäs, V. Moilanen, S. Helisalmi, M. Hiltunen, A. M. Remes, L. Q. Zhu, Novel Rare SORL1 Variants in Early-Onset Dementia. *J. Alzheimers. Dis.* **82**, 761–770 (2021).
45. S. Balduzzi, G. Rücker, G. Schwarzer, How to perform a meta-analysis with R: a practical tutorial. *Evid. Based. Ment. Health* **22**, 153–160 (2019).
46. A. M. Bolger, M. Lohse, B. Usadel, Trimmomatic: a flexible trimmer for Illumina sequence data. *Bioinformatics* **30**, 2114–2120 (2014).
47. A. Dobin, C. A. Davis, F. Schlesinger, J. Drenkow, C. Zaleski, S. Jha, P. Batut, M. Chaisson, T. R. Gingeras, STAR: ultrafast universal RNA-seq aligner. *Bioinformatics* **29**, 15–21 (2013).
48. Y. Liao, G. K. Smyth, W. Shi, The R package Rsubread is easier, faster, cheaper and better for alignment and quantification of RNA sequencing reads. *Nucleic Acids Res.* **47**, e47 (2019).
49. M. I. Love, W. Huber, S. Anders, Moderated estimation of fold change and dispersion for RNA-seq data with DESeq2. *Genome Biol.* **15**, 550 (2014).
50. H. Braak, I. Alafuzoff, T. Arzberger, H. Kretzschmar, K. Tredici, Staging of Alzheimer disease-associated neurofibrillary pathology using paraffin sections and immunocytochemistry. *Acta Neuropathol.* **112**, 389–404 (2006).
51. M. Marttinen, J. Paananen, A. Neme, V. Mitra, M. Takalo, T. Natunen, K. M. A. Paldanius, P. Mäkinen, M. Bremang, M. I. Kurki, T. Rauramaa, V. Leinonen, H. Soininen, A. Haapasalo, I. Pike, M. Hiltunen, A multiomic approach to characterize the temporal sequence in Alzheimer's disease-related pathology. *Neurobiol. Dis.* **124**, 454–468 (2019).
52. H. Martiskainen, J. Viswanathan, N. P. Nykänen, M. Kurki, S. Helisalmi, T. Natunen, T. Sarajärvi, K. M. A. Kurkinen, J. P. Pursiheimo, T. Rauramaa, I. Alafuzoff, J. E. Jääskeläinen, V. Leinonen, H. Soininen, A. Haapasalo, H. J. Huttunen, M. Hiltunen, Transcriptomics and mechanistic elucidation of Alzheimer's disease risk genes in the brain and in vitro models. *Neurobiol. Aging* **36**, 1221.e15-1221.e28 (2015).
53. T. Natunen, H. Martiskainen, T. Sarajaŕvi, S. Helisalmi, J. P. Pursiheimo, J. Viswanathan, M. Laitinen, P. Maḱinen, T. Kauppinen, T. Rauramaa, V. Leinonen, I. Alafuzoff, A. Haapasalo, H. Soininen, M. Hiltunen, Effects of NR1H3 genetic variation on the expression of liver X receptor α and the progression of Alzheimer's disease. *PLoS One* **8,** e80700 (2013).
54. T. Natunen, H. Martiskainen, M. Marttinen, S. Gabbouj, H. Koivisto, S. Kemppainen, S. Kaipainen, M. Takalo, H. Svobodová, L. Leppänen, B. Kemiläinen, S. Ryhänen, T. Kuulasmaa, E. Rahunen, S. Juutinen, P. Mäkinen, P. Miettinen, T. Rauramaa, J. Pihlajamäki, A. Haapasalo, V. Leinonen, H. Tanila, M. Hiltunen, Diabetic phenotype in mouse and humans reduces the number of microglia around β-amyloid plaques. *Mol. Neurodegener.* **15**, 66 (2020).
55. S. Kemppainen, N. Huber, R. M. Willman, A. Zamora, P. Mäkinen, H. Martiskainen, M. Takalo, A. Haapasalo, T. Sobrino, M. A. González Gómez, Y. Piñeiro, J. Rivas, U. Himmelreich, M. Hiltunen, Organotypic Hippocampal Slice Cultures from Adult Tauopathy Mice and Theragnostic Evaluation of Nanomaterial Phospho-TAU Antibody-Conjugates. *Cells* **12**, 1422 (2023).
56. S. Gabbouj, T. Natunen, H. Koivisto, K. Jokivarsi, M. Takalo, M. Marttinen, R. Wittrahm, S. Kemppainen, R. Naderi, A. Posado-Fernández, S. Ryhänen, P. Mäkinen, K. M. A. Paldanius, G. Doria, P. Poutiainen, O. Flores, A. Haapasalo, H. Tanila, M. Hiltunen, Intranasal insulin activates Akt2 signaling pathway in the hippocampus of wild-type but not in APP/PS1 Alzheimer model mice. *Neurobiol. Aging* **75**, 98–108 (2019).

57. H. Martiskainen, S. Helisalmi, J. Viswanathan, M. Kurki, A. Hall, S. K. Herukka, T. Sarajärvi, T. Natunen, K. M. A. Kurkinen, J. Huovinen, P. Mäkinen, M. Laitinen, A. M. Koivisto, K. M. Mattila, T. Lehtimäki, A. M. Remes, V. Leinonen, A. Haapasalo, H. Soininen, M. Hiltunen, Effects of Alzheimer's disease-associated risk loci on cerebrospinal fluid biomarkers and disease progression: a polygenic risk score approach. *J. Alzheimers. Dis.* **43**, 565–573 (2015).

Acknowledgement
The authors thank the BICeL platform of the Institut Biologie de Lille and the Vect'viral platform (INSERM US 005 – CNRS 3427 – TBMCore, Université de Bordeaux, France). The authors thank Karine Blary at the IEMN Lille for the microfabrication work.
The authors also thank Sisko Juutinen, Eija Rahunen, and Minna Turunen for excellent technical support with immunohistochemistry. Fluorescent microscopy of human brain samples was carried out with the support of UEF Cell and Tissue Imaging Unit, University of Eastern Finland, Finland.

Funding
JPND (JPND2019-466-128, project PGM-AD)
ANR (GENSYNALZ; ANR-21-CE16-0010)
Fondation Alzheimer (grant number 903716)
Fondation Claude Pompidou
Fondation pour la Recherche Médicale (ALZ201912009628)
Fondation Recherche Alzheimer
the French RENATECH network (P-18-02737)
Lille Métropole Communauté Urbaine and the French government's LABEX DISTALZ program (Development of innovative strategies for a transdisciplinary approach to Alzheimer's disease).
European Union under the European Regional Development Fund (ERDF)
Hauts de France Regional Council (contract469 no.18006176)
MEL (contract_18006176), and the French State (contract no. 2018-3-470 CTRL_IPL_Phase2).
Research Council of Finland (grant number 330178, 338182, 355604, 334802)
the Sigrid Jusélius Foundation
the Strategic Neuroscience Funding of the University of Eastern Finland, Faculty of Health Sciences of University of Eastern Finland
Alzheimer's Association (ADSF-24-1284326-C and AARG-22-926152).

Author's Contribution
Conceptualization: J.C., J.D.; J-C.L.
High content screening: A.C., T.M., D.K., J.C., J-C.L.;
Cell culture experiments: A.C., F.R., D.S-W., A.R.M.F., C.N., N.L-W., A. F-R., C.G., E.L., A-M.A, F.D., M.R.C., D.K., J.D.
Electrophysiological analyses: A.R., A.E., S.D., C.M.;
Immunohistochemistry and RNAseq analyses: L-I.C., M.T., H.M., R.M.W., H.J., P.M., S.H., M.Hil.;
WES sequencing data: M.Hul., P.A., C.C., O.D-I., H.J., T.K., M.K., J.H., S.H., H.H., P.M., G.N., S.M., M.W., A.R., T.R., A.P., R.S., H.S., J.V.S., J.W., R.M.W., J-C.L.;
Genetic Analysis: M.Hul., T.R., B.G-B., M.Hil., J-C.L.
Writing: A.C., F.R., M.T., A.R., H.M., D.K., C.M., J.C., M.Hil., J.D., J-C.L.

Conflicts of interest:
None

Availability of data and material
Cellular models used and/or analyzed in the current study are available from the corresponding authors upon request.

Figure 1. High-content screening identified nine AD-associated genes that significantly impact synaptic density and function in rat primary neurons. **(a-b)** Impact of shRNA-mediated downregulation of 198 AD-associated genes on synaptic density in rat hippocampal primary neuronal cultures (PNCs), virally transduced at MOI 2 **(a)** and MOI 4 **(b)**. Data given as mean±SEM, n=3, top and bottom 2.5% genes are shown in red. **(c)** Quantification of synapse density following the assignment of Homer1 to Syp spots on Map2-positive dendrites. Data given as mean±SEM, n=3. **(d-e)** Representative images of Map2, Syp and Homer1 immunostainings following shRNA-mediated downregulation of *Syp, Psmc3, Plcg2, Cyb561, Snx1, Ical1,* and *Nck2* at MOI 2 **(c)** and of *Syp, Csnk1g1, Usp6nl, Oplah* and *Nck2* at MOI 4 **(d)**; Scale bars = 20 µm. **(f)** Western blots showing the validation of gene downregulation for Usp6nl, Psmc3, Plcγ2, Csnk1g1, Cybk1g1, Cyb561, Snx1, Ica1l, Oplah, and Nck2 transduced at MOI 2 in PNCs. **(g)** Quantification of protein levels in PNCs transduced with these nine shRNAs, normalized by the non-targeting control (shNT) levels. Data given as mean±SD, n=3. **(h-i)** Impact of these nine shRNAs on the mean spike **(h)** and burst frequencies **(i)** in PNCs at DIV21, measured by MEA. Violin plots show median and quartile lines, n=3.
All statistical analyses were performed using Mann-Whitney test. *p<0.05, ** p<0.01, *** p<0.001.

Figure 2: *Plcg2* downregulation alters the morphology of DG granule cells. **(a)** Schematic representation of the experimental approach to downregulate *Plcg2* in the DG. The lentiviral constructs were injected by sterotaxy in either the ipsi- (LV-shPLCG2 for knock-down of *Plcg2*) or contralateral (LV-shNT, control) hemispheres. **(b)** High magnification immunofluorescence images of transduced DG cells as indicated by GFP expression, as well as a portion of dendritic branch with spines (control shNT left; shPLCG2 right); scale bars = 20 µm for left panels and 7 µm for right panels. **(c-f)** Measurements of dendritic length **(c)**, dendritic volume **(d)**, complexity index **(e)**, and branch number **(f)** in transduced DG granule cells. **(g)** Schematic diagram of the Sholl analysis illustrating the morphological change in the dendritic tree of representative control (grey) vs shPLCG2 (red) transduced DG granule cells. Scale bar = 20 µm. **(h)** Distribution of intersections based on the Sholl analysis. **(i-k)** Graphs comparing average spine density **(i)**, spine length **(j)** and spine head diameter **(k)**, indicating a marked alteration in synaptic contacts onto DG granule cells. Data expressed as mean±SEM for bar graphs with individual data points.
All statistical analyses were performed using Mann-Whitney test (for Sholl analysis n ≥90 per condition. * p<0.05, **** p<0.0001

Figure 3: *PLCG2* downregulation in DG granule cells leads to decreased excitability and reduced mEPSC frequency and amplitude. (a) Representative image of maximum intensity projection of section labeled with iba-1 (in magenta) and GFP (in green) showing the selective expression of viral vector in DG granule cells. MolDG= molecular layer of DG, GrDG= granular DG, PoDG= polymorph layer of DG. Patch-clamp recordings were performed from GFP expressing granule cells identified under the electrophysiology microscope. Scale bar = 10 µm. **(b)** Representative traces from shNT (in grey) and shPLCG2 (in red) transduced DG granule cells recorded in the current-clamp mode, with injection of current steps from –80 pA to 0 pA with 10 pA increments. **(c)** Representative traces of current-clamp recordings showing spike discharges triggered by a depolarization pulse of current (120 pA) from shNT (in grey) and shPLCG2 (in red) transduced DG cells. **(d-f)** Current-clamp recordings were used to assess input resistance **(d)**, resting membrane potential (RMP) **(e)** and rheobase **(f)**. **(g)** Number of spikes plotted against current injected. **(h)** Representative traces of miniature excitatory post-synaptic currents (mEPSCs) recorded in the voltage-clamp mode from shNT (in grey) and shRNA (in red) DG cells in presence of 500 nM TTX. **(i-k)** Measurements of average frequency of mEPSCs **(i),** average amplitude of mEPSCs **(j)** and cumulative distribution of mEPSC amplitudes **(k)**. Data are represented as mean±SEM with bar and individual data points for average values, where individual data points indicate each cell recorded; shNT n=27 and shRNA n=15 with scale bar for mEPSCs= 10pA/1s; for RMP and input resistance shNT n=15 and shRNA n=14 with scale 40mV/20mV.
All statistical analyses were performed using Mann-Whitney test at the exception of the cumulative distribution were a Kolmogorov-Smirnov (KS) test was applied. * p<0.05, ** p<0.01, ***p<0.001.

Figure 4. Downregulation of PLCγ2 in hNCs negatively impacts synapses and AD hallmarks
(a) Representative images of hNCs after 4 weeks of spontaneous differentiation from progenitors stably expressing either a non-targeting shRNA (shNT) or a shRNA targeting *PLCG2* (shPLCG2); scale bar = 20 µm. **(b)** Western blots showing the specificity of PLCγ2 downregulation via shPLCG2 in hNCs. **(c)** Immunofluorescence images of MAP2, SYP and HOMER1 synaptic markers in shNT- and shPLCG2-transduced hNCs at 4 weeks. Scale bar = 20 µm. **(d)** Synaptic marker densities for the two conditions. Data given as mean±SEM, n=3; **(e)** Impact of shPLCG2 on spike and burst frequencies in hNCs, measured via MEA. Violin plots show median and quartile lines, n=3; **(f)** Representative Western blots of APP, total Tau and Tau phosphorylated at T181, S202-T205, T217, T231 and S396-S404 in shNT- and shPLCG2-transduced hNCs; **(g)** Quantification of APP and TAU levels for the two conditions. Data given as mean ± SD, n=3; **(h)** Aβ peptides levels in shNT- or shPLCG2- transduced hNCs, measured by Alpha-LISA. Data given as means ± SEM, n=3; **(i)** Tau phosphorylation levels in hNCs expressing (or not) shPLCG2. Data given as mean ± SD, n=3; **(j)** Representative Western blots of total and phosphorylated forms of ERK1/2, GSK3β, P38-MAPK and AKT in shNT- and shPLCG2-transduced hNCs. **(k)** Quantification of total and phosphorylated protein levels for these targets in shNT- and shPLCG2-transduced hNCs. Data given as mean ± SD, n=3.
All statistical analyses were performed using Mann-Whitney test. *p<0.05, ***p<0.001, ****p<0.0001

Figure 5. The *PLCG2* p.Q816X and p.R953X non-sense variants increase AD risk and reduce *PLCG2* expression and PLCγ2 protein levels, consistently with a protective effect of PLCG2 re-expression in shPLCG2-hNCs. (a) Meta-analysis of the ADGEN and ADES Whole Exome Sequencing data **(b)** Western blot of the post-mortem brain tissue of an AD patient carrying the p.R953X variant in comparison with four other AD cases. **(c)** Quantification of PLCγ2 protein levels in these samples. **(d)** RNAseq showing a 40% decrease in the blood *PLCG2* mRNA expression in the p.Q816X carrier as compared to the average of matched control group (n=4). **(e)** Representative Western blots of APP, total and T231-phospho-Tau total and phospho-GSK3β, and total and phospho-AKT protein levels in shNT-hNCs, shPLCG2-hNCs, and shPLCG2-hNCs overexpressing PLCG2. Quantification of APP and Tau protein levels **(f),** Aβ peptides levels in the culture medium measured by Alpha-LISA and normalized to total protein levels **(g)** and Tau phosphorylated levels at T231 (normalized by total Tau) **(h)** in shNT-hNCs, shPLCG2-hNCs, and shPLCG2-hNCs overexpressing PLCG2**.** For these groups. Data given as mean ± SD, n=3. **(i)** Representative images of T231-phospho-Tau, total Tau, and MAP2 immunostainings in shNT-hNCs, shPLCG2-hNCs, and shPLCG2-hNCs overexpressing PLCG2. Scale bar = 20 µm. **(j)** Quantification of T231-pTAU in the neuronal somata for these groups. Data given as mean ± SEM, n=3. **(k)** Changes in total and phospho-protein levels for GSK3β and AKT in shNT-hNCs, shPLCG2-hNCs, and shPLCG2-hNCs overexpressing PLCγ2. Data given as mean ± SD, n=3.
All statistical analyses were performed using Mann-Whitney test. *p<0.05.

Figure 1.

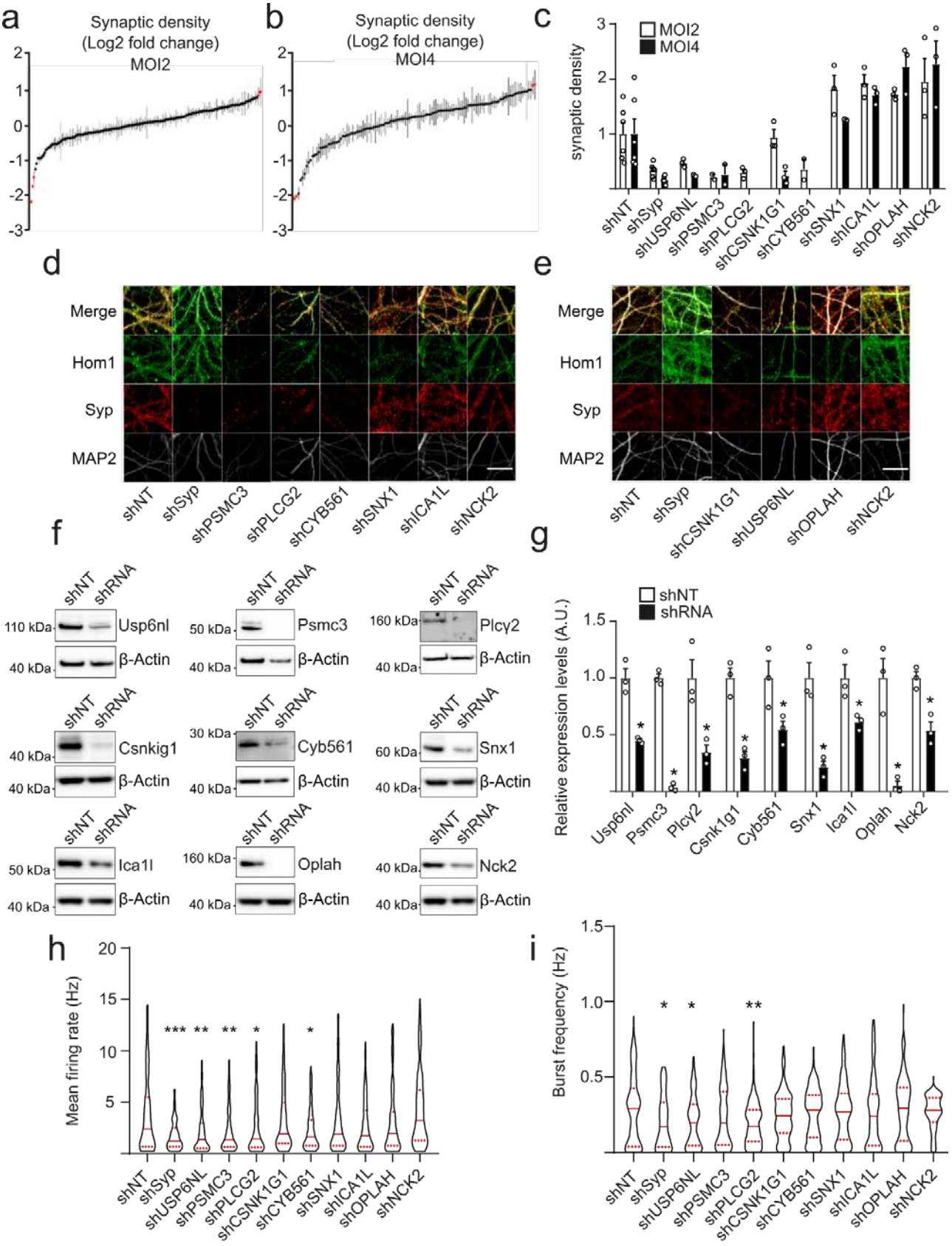
a
Synaptic density
(Log2 fold change)
MOI2
b
Synaptic density
(Log2 fold change)
MOI4
c
MOI2
MOI4
synaptic density
shNT
shSyp
shUSP6NL
shPSMC3
shPLCG2
shCSNK1G1
shCYB561
shSNX1
shICA1L
shOPLAH
shNCK2
d
Merge
Hom1
Syp
MAP2
shNT
shSyp
shPSMC3
shPLCG2
shCYB561
shSNX1
shICA1L
shNCK2
e
Merge
Hom1
Syp
MAP2
shNT
shSyp
shCSNK1G1
shUSP6NL
shOPLAH
shNCK2
f
shNT
shRNA
Usp6nl
Psmc3
Plcγ2
Csnkig1
Cyb561
Snx1
Ica1l
Oplah
Nck2
β-Actin
g
shNT
shRNA
Relative expression levels (A.U.)
Usp6nl
Psmc3
Plcγ2
Csnk1g1
Cyb561
Snx1
Ica1l
Oplah
Nck2
h
Mean firing rate (Hz)
shNT
shSyp
shUSP6NL
shPSMC3
shPLCG2
shCSNK1G1
shCYB561
shSNX1
shICA1L
shOPLAH
shNCK2
i
Burst frequency (Hz)
shNT
shSyp
shUSP6NL
shPSMC3
shPLCG2
shCSNK1G1
shCYB561
shSNX1
shICA1L
shOPLAH
shNCK2

Figure 2.

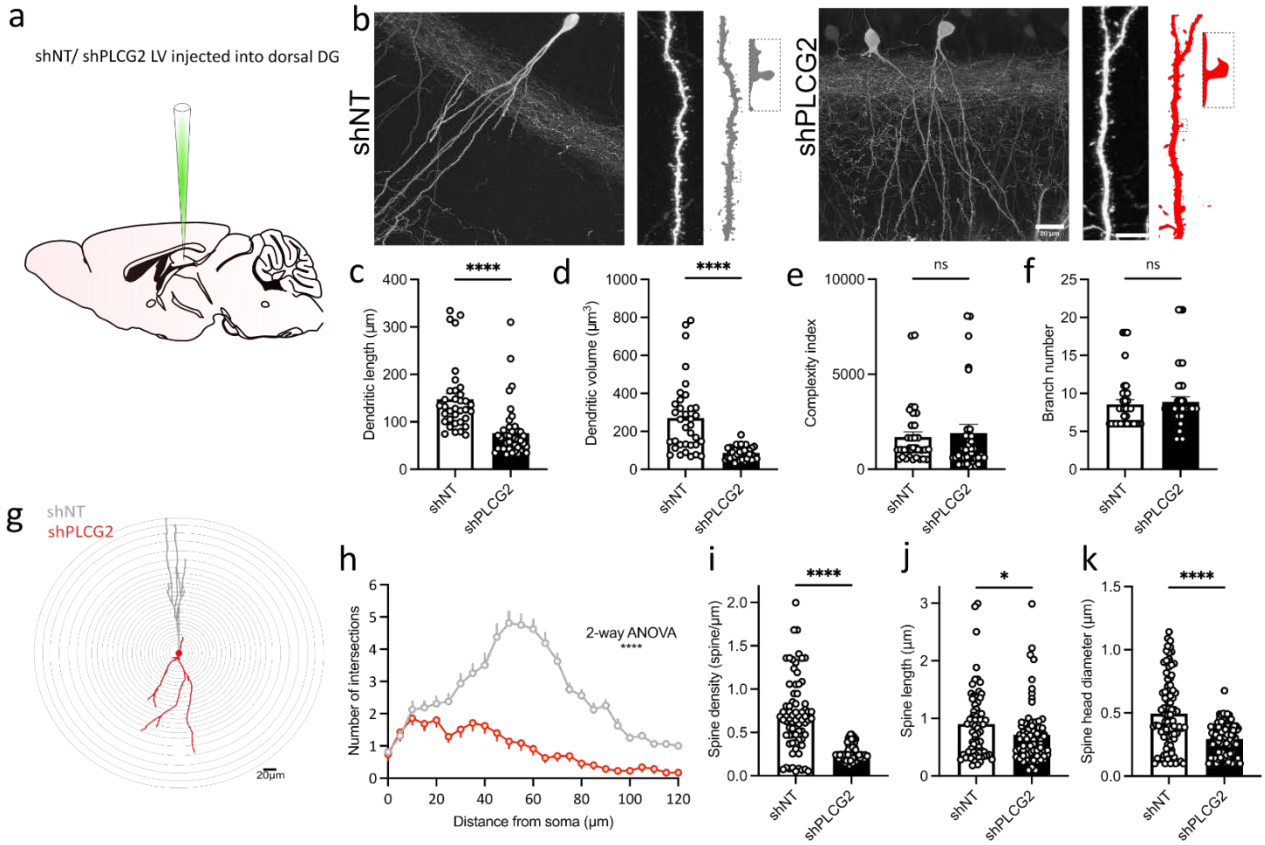
a
shNT/ shPLCG2 LV injected into dorsal DG
b
shNT
shPLCG2
c
Dendritic length (µm)
****
d
Dendritic volume (µm³)
****
e
Complexity index
ns
f
Branch number
ns
shNT
shPLCG2
g
shNT
shPLCG2
20µm
h
Number of intersections
2-way ANOVA
****
Distance from soma (µm)
i
Spine density (spine/µm)
****
j
Spine length (µm)
*
k
Spine head diameter (µm)
****

Figure 3.

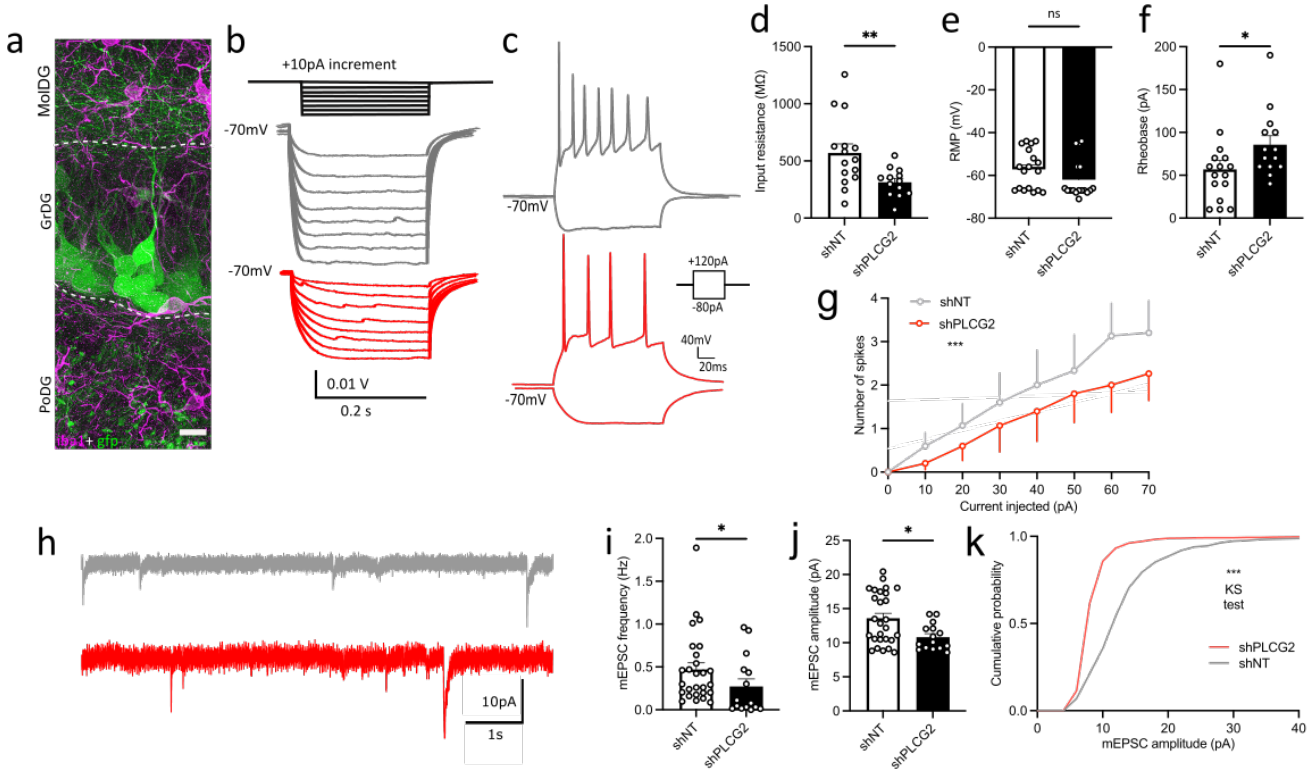
a
MolDG
GrDG
PoDG
b
+10pA increment
-70mV
-70mV
0.01 V
0.2 s
c
-70mV
+120pA
-80pA
40mV
20ms
-70mV
d
Input resistance (MΩ)
**
shNT
shPLCG2
e
RMP (mV)
ns
shNT
shPLCG2
f
Rheobase (pA)
*
shNT
shPLCG2
g
shNT
shPLCG2
***
Number of spikes
Current injected (pA)
h
10pA
1s
i
mEPSC frequency (Hz)
*
shNT
shPLCG2
j
mEPSC amplitude (pA)
*
shNT
shPLCG2
k
Cumulative probability
***
KS
test
shPLCG2
shNT
mEPSC amplitude (pA)

Figure 4.

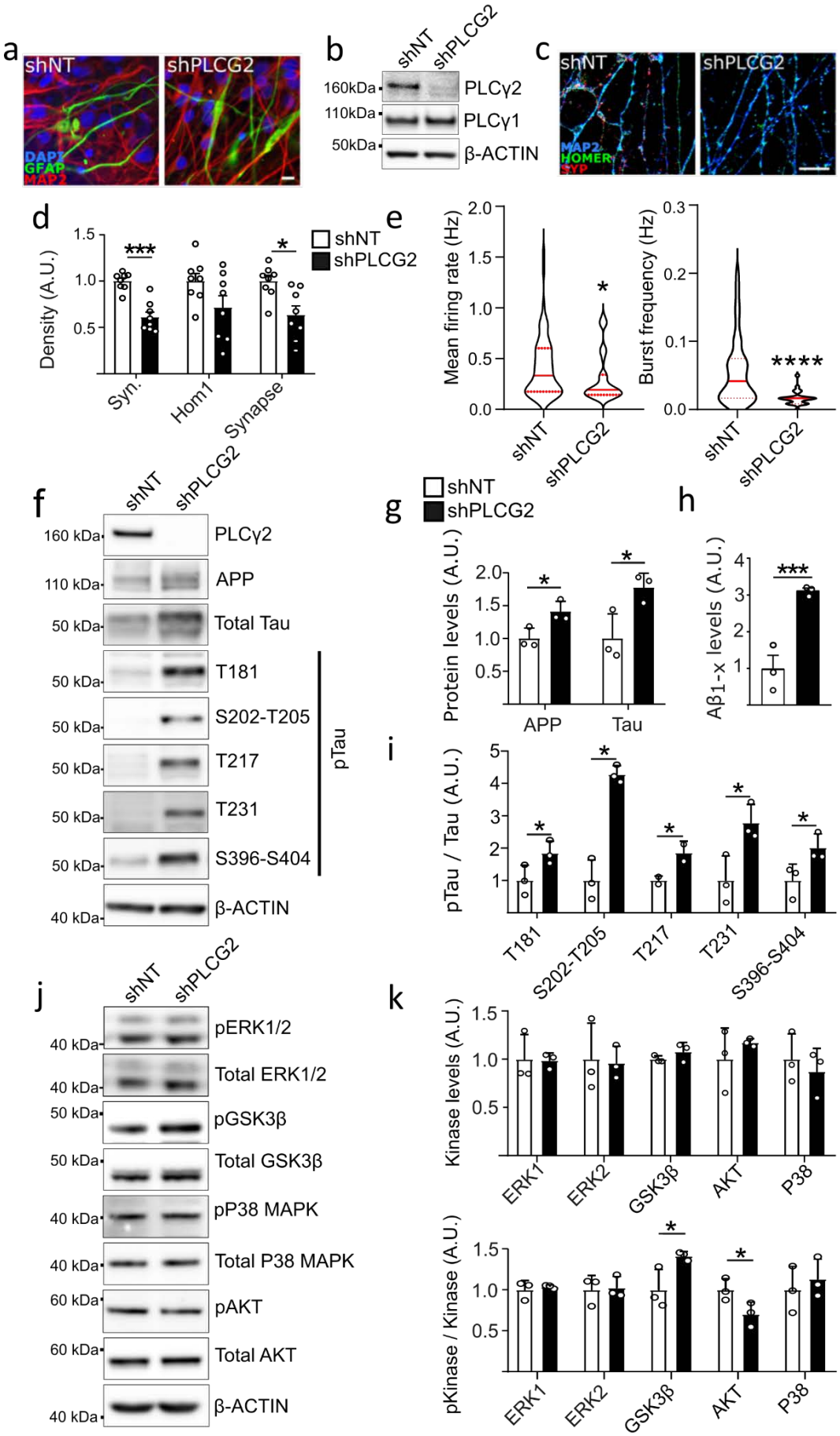
a
shNT
shPLCG2
DAPI
GFAP
MAP2
b
shNT
shPLCG2
160kDa
110kDa
50kDa
PLCγ2
PLCγ1
β-ACTIN
c
shNT
shPLCG2
MAP2
HOMER
SYP
d
Density (A.U.)
1.5
1.0
0.5
***
*
shNT
shPLCG2
Syn.
Hom1
Synapse
e
Mean firing rate (Hz)
2.0
1.5
1.0
0.5
0.0
*
Burst frequency (Hz)
0.3
0.2
0.1
0.0
****
shNT
shPLCG2
f
shNT
shPLCG2
160 kDa
110 kDa
50 kDa
PLCγ2
APP
Total Tau
T181
S202-T205
T217
T231
S396-S404
pTau
β-ACTIN
40 kDa
g
shNT
shPLCG2
Protein levels (A.U.)
2.0
1.5
1.0
0.5
*
APP
Tau
h
Aβ1-x levels (A.U.)
4
3
2
1
***
i
pTau / Tau (A.U.)
5
4
3
2
1
T181
S202-T205
T217
T231
S396-S404
j
shNT
shPLCG2
40 kDa
pERK1/2
Total ERK1/2
50 kDa
pGSK3β
Total GSK3β
pP38 MAPK
Total P38 MAPK
60 kDa
pAKT
Total AKT
β-ACTIN
k
Kinase levels (A.U.)
1.5
1.0
0.5
ERK1
ERK2
GSK3β
AKT
P38
pKinase / Kinase (A.U.)

Figure 5.

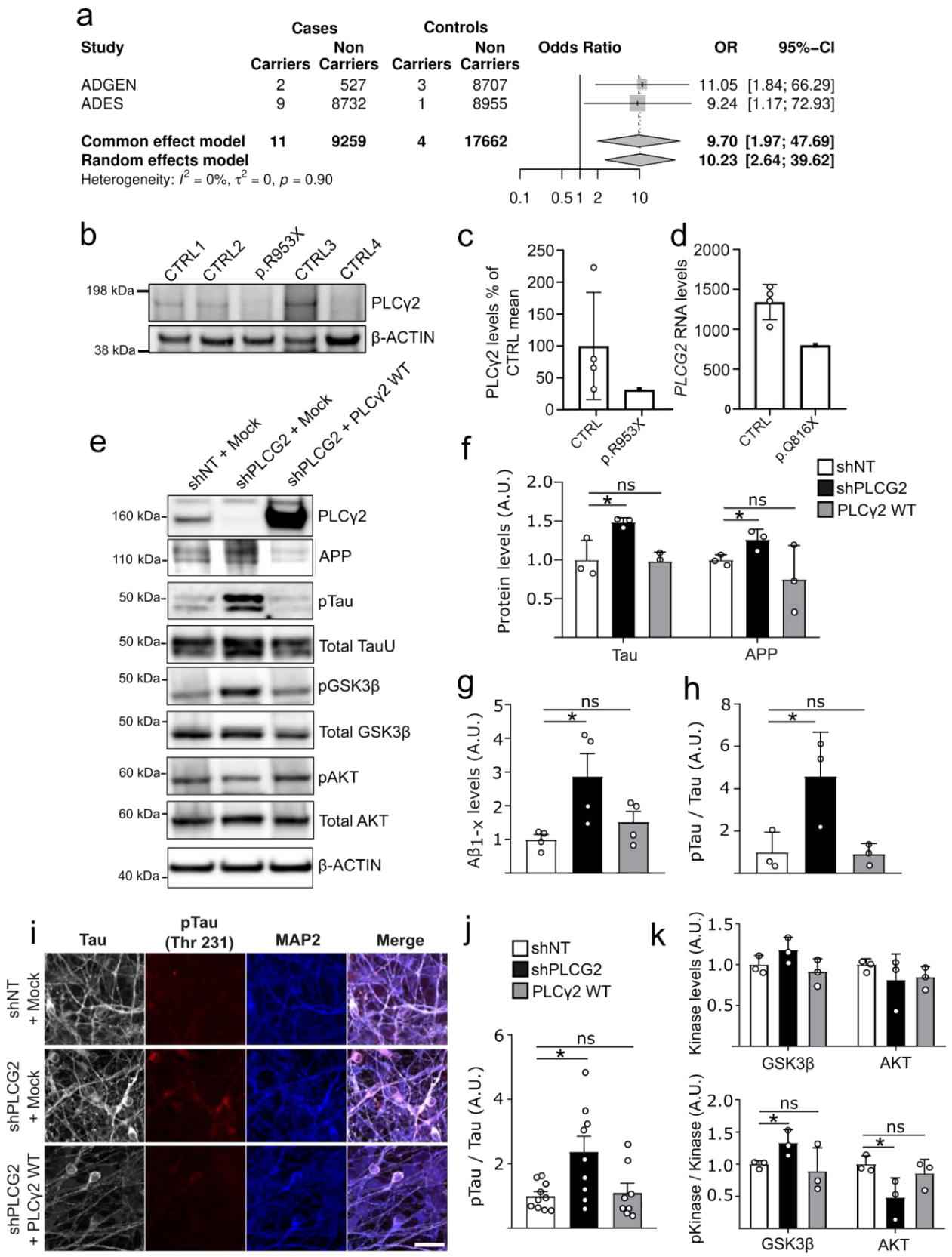
a
Cases
Controls
Study
Carriers
Non Carriers
Carriers
Non Carriers
Odds Ratio
OR
95%–CI
ADGEN 2 527 3 8707 11.05 [1.84; 66.29]
ADES 9 8732 1 8955 9.24 [1.17; 72.93]
Common effect model 11 9259 4 17662 9.70 [1.97; 47.69]
Random effects model 10.23 [2.64; 39.62]
Heterogeneity: I^2 = 0%, τ^2 = 0, p = 0.90
0.1 0.5 1 2 10
b
CTRL1
CTRL2
p.R953X
CTRL3
CTRL4
198 kDa
38 kDa
PLCγ2
β-ACTIN
c
PLCγ2 levels % of CTRL mean
CTRL
p.R953X
d
PLCG2 RNA levels
CTRL
p.Q816X
e
shNT + Mock
shPLCG2 + Mock
shPLCG2 + PLCγ2 WT
160 kDa PLCγ2
110 kDa APP
50 kDa pTau
50 kDa Total TauU
50 kDa pGSK3β
50 kDa Total GSK3β
60 kDa pAKT
60 kDa Total AKT
40 kDa β-ACTIN
f
shNT
shPLCG2
PLCγ2 WT
Protein levels (A.U.)
ns
*
Tau
APP
g
Aβ1-x levels (A.U.)
h
pTau / Tau (A.U.)
i
Tau
pTau (Thr 231)
MAP2
Merge
shNT + Mock
shPLCG2 + Mock
shPLCG2 + PLCγ2 WT
j
shNT
shPLCG2
PLCγ2 WT
pTau / Tau (A.U.)
k
Kinase levels (A.U.)
GSK3β
AKT
pKinase / Kinase (A.U.)